

塔里木盆地北部富满地区超深层走滑断裂带碳酸盐岩 油气差异成藏成因探讨

乔俊程^{1,2},常少英^{1,3},曾溅辉^{1,2},曹鹏³,董科良^{1,2},王孟修³,杨冀宁^{1,2},刘亚洲^{1,2},隆辉^{1,2},
安廷⁴,杨睿⁵,文林^{1,2}

[1. 中国石油大学(北京)油气资源与探测国家重点实验室,北京102249;2. 中国石油大学(北京)地球科学学院,北京102249;

3. 中国石油杭州地质研究院,浙江杭州310023;4. 中国石油新疆油田分公司,新疆克拉玛依834000;

5. 北京大学地球与空间科学学院,北京100871]

摘要:塔里木盆地北部超深层走滑断裂体系海相碳酸盐岩油气勘探开发近年来取得了重大突破,但富满油田油气分布与富集特征差异显著,走滑断裂控制下的超深层油气差异成藏机理尚不清楚。研究了富满地区走滑断裂几何结构及其演化过程,探讨其在油气运聚成藏中的作用,分析油气成藏富集机理,提出了油气富集主控因素。研究结果表明:①研究区走滑断裂经历了早期伸展或弱挤压,中期压扭、伸展或平移走滑,晚期定型、继承发育或张扭反转的动力学演化过程。 F_5 断裂带和 F_{17} 断裂带挤压、剪切和拉张应力交替发育,不同部位演化差异明显, F_7 断裂带和 F_{16} 断裂带以剪切应力和拉张应力为主,演化过程相对简单。②演化过程不同的断裂形成了不同的几何结构,造成通源性、输导性与储集性强弱差异配置不同,从而形成了3种不同的油气充注方式。 F_5 断裂带和 F_{16} 断裂带油气以垂向充注为主, F_7 断裂带油气以侧向运移调整为主, F_{17} 断裂带为垂向充注-侧向运移复合型。③断裂演化过程差异控制了油气充注过程。东部断裂晚期活动性强,喜马拉雅期高成熟裂解气大量充注成藏,形成了“西油东气”的格局。断裂带内不同部位演化过程差异加剧了断裂内油气性质变化的复杂性。④垂向充注型油气藏中通源性、输导性和储集性的耦合配置关系控制了油气富集程度,充注期次差异控制了油气性质变化,油气侧向运移为主的油气藏中储集性及侧向连通程度控制了油气富集程度及油气性质的变化。

关键词:运聚能力;成藏富集机理;走滑断裂;超深层;碳酸盐岩油气藏;富满地区;塔里木盆地

中图分类号:TE122.3 文献标识码:A

Origin of differential hydrocarbon accumulation in ultra-deep carbonate reservoirs along strike-slip fault zones in the Fuman area, northern Tarim Basin

QIAO Juncheng^{1,2}, CHANG Shaoying^{1,3}, ZENG Jianhui^{1,2}, CAO Peng³, DONG Keliang^{1,2}, WANG Mengxiu³,
YANG Jining^{1,2}, LIU Yazhou^{1,2}, LONG Hui^{1,2}, AN Ting⁴, YANG Rui⁵, WEN Lin^{1,2}

[1. State Key Laboratory of Petroleum Resources and Engineering, China University of Petroleum (Beijing), Beijing 102249, China;

2. College of Geosciences, China University of Petroleum (Beijing), Beijing 102249, China; 3. Hangzhou Research Institute of Geology,

PetroChina, Hangzhou, Zhejiang 310023, China; 4. Xinjiang Oilfield Company, PetroChina, Karamay, Xinjiang 834000, China;

5. School of Earth and Space Sciences, Peking University, Beijing 100871, China]

Abstract: In recent years, breakthroughs have been achieved in hydrocarbon exploration efforts in the ultra-deep marine carbonate rocks of strike-slip fault systems in the northern Tarim Basin. However, the Fuman oilfield in the basin exhibits pronounced differences in hydrocarbon distribution and enrichment, with the mechanisms driving the differential hydrocarbon accumulation in ultra-deep reservoirs governed by strike-slip faults remaining unclear. In this study, we investigate the geometric structures and evolution of strike-slip faults in the Fuman area, as well as their role

收稿日期:2024-05-22;修回日期:2024-09-12。

第一作者简介:乔俊程(1991—),男,副教授,油气成藏机理与非常规油气地质评价。**E-mail:** Juncheng.Qiao@cup.edu.cn。

通信作者简介:曾溅辉(1962—),男,教授,油气成藏机理与含油气盆地流体分析。**E-mail:** zengjh@cup.edu.cn。

基金项目:国家自然科学基金企业创新发展联合基金项目(U21B2063);国家自然科学基金青年基金项目(42302144);中央高校基本科研业务经费项目(2462023BJRC012)。

in hydrocarbon migration and accumulation. By analyzing the hydrocarbon accumulation and enrichment mechanisms, we identify the dominant factors controlling hydrocarbon accumulation in ultra-deep carbonate reservoirs in the area. The results indicate that the strike-slip faults in the study area experienced a dynamic evolutionary process consisting of the early extension or weak compression, the middle-stage transpression, extension, or translation slip, and the late-stage stabilization, successive development, or tensile-shear inversion. The F₅ and F₁₇ fault zones underwent alternating compression, shear, and tensile stresses, resulting in significant evolutionary differences across their various parts. In contrast, the F₇ and F₁₆ fault zones were primarily subjected to shear and tensile stresses, leading to relatively simple evolutionary processes. The faults with differential evolutionary processes exhibit distinct geometric structures, resulting in varying configurations of their connection to source rocks, hydrocarbon transport capacities, and reservoir properties. Consequently, three hydrocarbon charging models are formed: vertical charging as represented by F₅ and F₁₆, lateral migration for adjustment by F₇, and a combination of the former two patterns by F₁₇. The hydrocarbon charging process is governed by the differential evolution of fault zones. The late-stage strong activity of faults in the eastern part of the Fuman area, combined with the charging and accumulation of substantial highly mature pyrolysis gas during the Himalayan movement, results in the formation of a hydrocarbon distribution pattern characterized by “oil in the west and gas in the east”. Furthermore, the evolutionary differences across various parts of the fault zones cause more complex changes in hydrocarbon properties. For reservoirs dominated by vertical hydrocarbon charging, the degree of hydrocarbon enrichment is determined by the coupling of the connection to source rocks, hydrocarbon transport capacities, and reservoir properties of fault zones. Meanwhile, the hydrocarbon properties of the reservoirs are governed by the various hydrocarbon charging stages. For reservoirs dominated by lateral hydrocarbon migration, the degree of hydrocarbon enrichment and hydrocarbon property changes are controlled by their properties and the extent of lateral connections within.

Key words: migration and accumulation capacity, enrichment mechanism, strike-slip fault, ultra-deep reservoir, carbonate hydrocarbon reservoir, Fuman area, Tarim Basin

引用格式: 乔俊程,常少英,曾溅辉,等. 塔里木盆地北部富满地区超深层走滑断裂带碳酸盐岩油气差异成藏成因探讨[J]. 石油与天然气地质,2024, 45(5):1226–1246. DOI: 10.11743/ogg20240503.

QIAO Juncheng, CHANG Shaoying, ZENG Jianhui, et al. Origin of differential hydrocarbon accumulation in ultra-deep carbonate reservoirs along strike-slip fault zones in the Fuman area, northern Tarim Basin[J]. Oil & Gas Geology, 2024, 45(5):1226–1246. DOI: 10.11743/ogg20240503.

近年来,国内外超深层(埋深>6 000 m)油气勘探发展迅速,北美、俄罗斯、欧洲及中东地区发现了上百个超深层油气藏,超深层中探明的石油和天然气储量分别占全球油气探明储量增量的13%和21%^[1-3]。近10年来,中国超深层油气勘探开发进入快速发展阶段,在四川盆地和塔里木盆地埋深大于6 000 m的前寒武系-下古生界古老海相碳酸盐岩地层中取得了重大的油气突破,建成了安岳气田及哈拉哈塘、顺北和富满等多个大型油田^[2-6]。

塔里木盆地顺北地区和富满地区油气勘探深度超过8 000 m,超深层油气的形成和调整十分活跃^[5-8]。盆地超深层海相地层油气当量约70×10⁸ t,年产量峰值超过370×10⁴ t。盆地早期勘探以构造高部位为主,在塔北隆起和塔中凸起奥陶系发现了多个岩溶型油气藏,前人研究提出了沉积微相和岩溶作用共同控制油气储层分布的油气成藏模式^[4, 7, 9]。塔

北凹陷富满油田和顺北油田的勘探发现揭示了走滑断裂体系对超深层奥陶系碳酸盐岩油气藏的重要影响。研究认为,走滑断裂具有明显的“控储、控藏、控富”作用^[10-15]。塔北地区奥陶系油气藏油气性质差异大,油气分布与富集规律复杂,国内外学者围绕走滑断裂的成藏机制开展了走滑断裂特征、活动性及其演化,走滑断裂对油气储层的控制和改造,以及油气成藏期次、油气来源、油气运移等多个方面的研究^[16-30]。

有效储集体及与之相关的油气运聚输导体系是超深层油气成藏研究的核心内容。在塔北凹陷,走滑断裂不仅控制了奥陶系白云岩和灰岩储层的储集性能,也是沟通寒武系玉尔吐斯组烃源岩的纽带^[4, 10-12, 18-20, 28]。因此,走滑断裂特征与演化及其对油气藏形成与分布的控制和影响是该区油气藏成藏机理研究的关键^[7, 9, 25, 31]。已有研究表明,在不同类型的走滑断裂以及同一断裂的不同力学性质段,油气的运移和聚

集条件相差很大,主要体现在走滑断裂对深部烃源岩沟通程度、上部断溶储集体的发育规模和走滑断裂演化动力学过程3个方面^[6, 11, 12, 15, 15-23, 32-34]。中国学者从不同角度对油气藏形成和分布进行了探讨:①油气性质差异的形成原因^[6, 10, 15, 28-30, 38-39]。张水昌等(2021)认为烃源岩差异演化造成的多期油气充注及后期气洗作用是油气藏油气相态区别的主要原因^[8];赵永强等(2021)指出不同期次、不同性质的油气混合导致了奥陶系复杂的油气性质分布^[40];田军等(2021)认为富满地区烃源岩的生、排烃过程及油气充注期次是油气性质及其分布的重要控制因素^[9]。②油气分布和富集差异的主控因素。前人研究发现油气藏分布形态受走滑断裂储集体特征的影响,部分学者认为油气规模和富集程度与走滑断裂的力学分段密切相关,王清华等(2021)和汪如军等(2021)发现不同力学分段的油气输导作用强度不同,油气分布的部位和范围有区别^[31, 41]。走滑断裂带超深层碳酸盐岩油气藏油气性质、分布和富集的影响因素多样,并非受单一因素影响,而是受多要素的耦合控制,主控因素尚不清晰。

已有研究认为,走滑断裂带在超深层碳酸盐岩油气成藏中兼具通源、输导和储集3种作用,这3种作用的差异发育是油气藏分布和富集特征差异的主要原因,同时,走滑断裂的演化与活动过程影响了油气充注期次,对油气性质具有重要影响。本文以塔里木盆地北部阿满过渡带富满地区为研究对象,选取F₅, F₇, F₁₆和F₁₇等4条典型断裂带,在明确断裂带间与断裂带内油气性质、分布与富集程度差异的基础上,以断裂带几何结构刻画为基础,形成走滑断裂通源性、输导性和储集性的定量表征方法,揭示超深层油气藏油气成藏条件的配置关系。通过断裂演化动力学分析,确定油气成藏过程和油气运聚方式,揭示油气成藏与富集差异的主控因素。本文旨在深化超深层碳酸盐岩油气藏成藏机理,为超深层油气勘探开发提供借鉴。

1 研究区地质概况

塔里木盆地是中国最大的含油气叠合盆地,面积约为 $56 \times 10^4 \text{ km}^2$,由新生代前陆盆地和古-中生代克拉通盆地组成,构造上可以划分为塔北隆起带、北部坳陷带、中央隆起带、东南断隆带和西南坳陷带^[9, 18, 41](图1a,b)。富满地区主体位于北部坳陷带的阿满过渡带东部,处于裂陷-拗陷体系的沉降中心区^[10-11, 18, 41-42]。富满地区早寒武世早期沉积了一套厚

度在50~100 m的玉尔吐斯组暗色泥岩,中、晚寒武世—中奥陶世,发育了巨厚的海相碳酸盐岩地层,与晚奥陶世桑塔木组的巨厚陆棚泥岩形成优质的储-盖组合^[7, 20-24, 35](图1c)。目前,富满地区已发现的油气主要分布于埋深6 500~8 000 m的中奥陶统一间房组和鹰山组顶部,截至2020年,已探明石油地质储量 $1.02 \times 10^8 \text{ t}$ ^[7, 20-22]。

塔北—阿满—塔中地区走滑断裂多期活动、继承发育,表现出明显的分区、分带特征^[30, 33, 38, 44-46],阿满过渡带西部主要为NW向单剪走滑断裂体系,富满地区主要发育NE向的单剪走滑断裂体系(图1a)。多期活动的走滑断裂为富满地区的油气运移、聚集和富集提供了优越的成藏条件,是油气输导的路径,也是油气富集的场所^[9, 18, 41]。

2 走滑断裂带结构特征及演化过程

2.1 走滑断裂带几何结构特征及其差异

富满地区走滑断裂带表现出“平面分段、纵向分层”的特征^[10-11, 38, 47],平面上,按照力学性质均可划分为挤压段、平移段和拉分段^[17-18, 48]。F₅断裂带以挤压段为主;F₇断裂带和F₁₆断裂带平移段占主导,发育少量拉分段;F₁₇断裂带出现挤压、拉分和平移交替的特征(图2;图3a,f,k,p)。

纵向上,断裂在寒武系主要为直立线性构造,在奥陶系上部分支断裂发育,出现了正花状、负花状、复合花状和直立线性4种构造^[41](图3)。F₅断裂带在横向上从南向北出现负花状—正花状—负花状构造组合,以正花状为主,负花状为辅(图3a—d);F₇断裂带表现为正花状—负花状—正花状组合,以负花状为主(图3e—h);F₁₆断裂带以直立线性构造为主(图3i—l);F₁₇断裂带出现负花状—复合花状—正花状—直立线性的复杂变化(图3m—p)。

2.2 走滑断裂带间与断裂带内演化过程及其差异

在早、中寒武世演化早期,塔里木板块处于伸展应力背景下,内部形成伸展构造或小型断裂;晚寒武世—中奥陶世末演化中期,整个板块处于南北挤压应力场中,富满地区形成了以NE向为主、NW向为辅的X共轭走滑断裂体系,在中奥陶统形成分支断裂,形成了多种的花状构造;至晚奥陶世末,应力格局保持稳定,平面上小位移走滑断裂相互连接,形成大型走滑断裂;晚志留世—中泥盆世演化末期,北侧南天

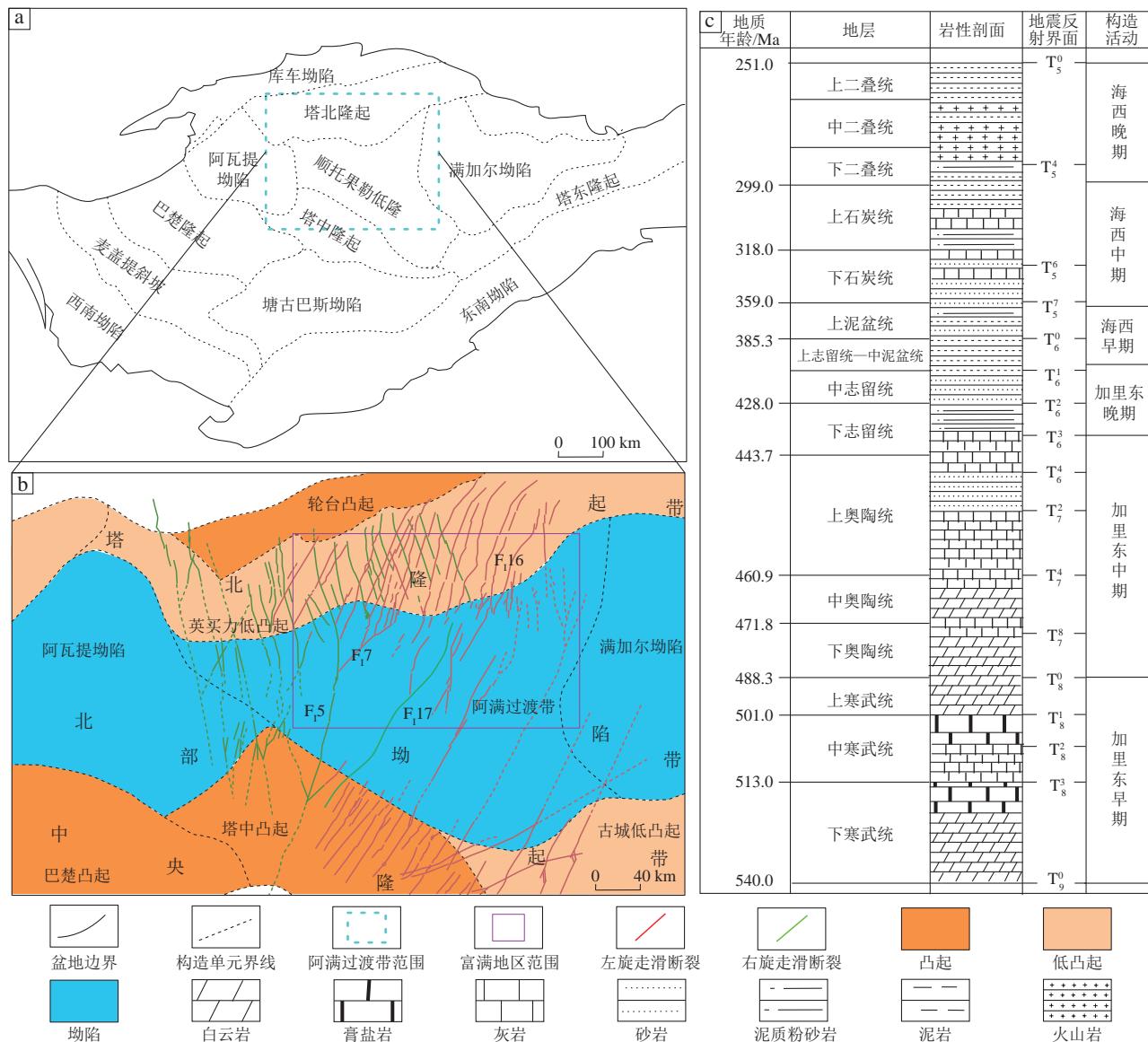


图1 富满地区地质概况

Fig. 1 Geological overview of the Fuman area

a. 塔里木盆地构造单元划分; b. 富满地区构造位置(据文献[18]修改); c. 地层柱状图(据文献[47]修改)

山洋逐渐闭合,应力场整体转变为NW-SE向,研究区部分断裂定型,部分断裂发生张扭反转,形成小型地堑构造^[15, 33, 46, 49-52](图4)。

断裂带间及断裂带内的走滑断裂演化过程存在差别^[42, 53]。F₅断裂带南部挤压段具有早期伸展、中期压扭走滑或伸展增强及晚期张扭反转定型的演化特征;在北部拉分段,断裂早期挤压形成小规模断层,中期压扭走滑,晚期定型(图4a—c)。F₁₇断裂带早期形成小型伸展断裂,中期满深2井和满深3井区发育压扭走滑,满深4井和满深5井区发育平移走滑,晚期这两个区域又分别发生张扭性反转和继承性活动(图4f,g)。F₇断裂带与F₁₆断裂带整体早期弱伸展,中期平移走滑,晚期断裂继承活动并定型(图4d,e)。

3 走滑断裂带油气成藏与富集差异

3.1 油气藏分布特征及其差异

富满地区奥陶系油气藏主要分布在基底深大断裂及与之相连的次级断裂附近,表现出“大断裂大油气藏,小断裂小油气藏”的特征^[7, 9, 27, 42]。油气藏主要分布在一间房组和鹰山组顶部,以构造-岩性油气藏为主,形成多个独立的油-水系统。F₅断裂带油气藏规模相对较大,南部油-水互层,北部油-干(层)互层(图5a);F₇断裂带油气藏规模相对小,以油-干互层为主(图5b);F₁₆断裂带油气藏规模也相对较小,南部以气层为主,北部出现

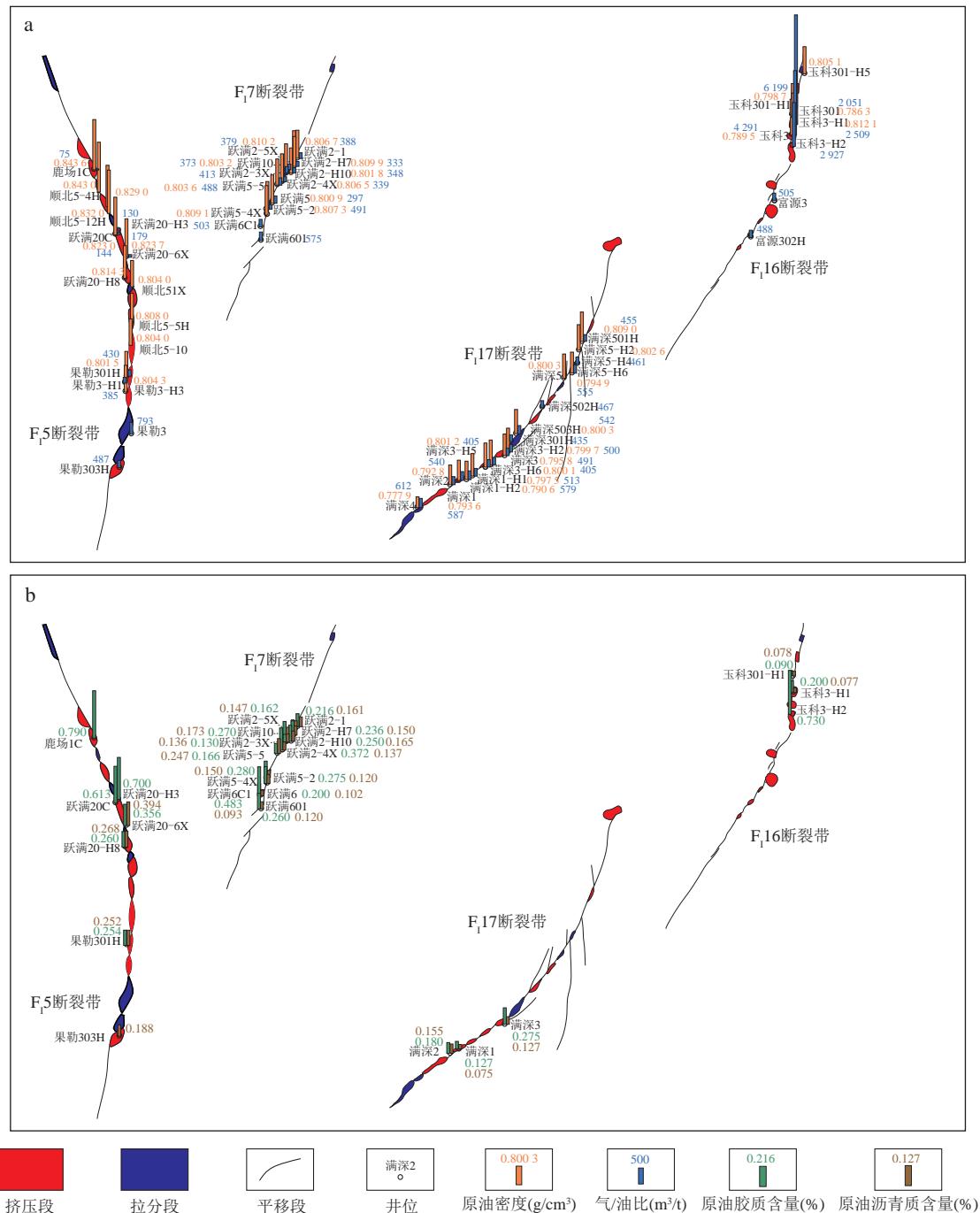


图2 富满地区典型断裂带平面分布特征及油气性质平面变化特征

Fig. 2 Maps showing typical fault zones and variation in hydrocarbon properties in the Fuman area

a. 原油密度与气/油比分布; b. 原油胶质与沥青质含量分布

含水气层(图5c); F_{17} 断裂带油藏规模较大,南部以油气层为主,北部出现油层(图5d)。

3.2 油气性质特征、变化规律及其差异

富满地区油气性质具有“西油东气、高重低轻”的变化特征^[9, 43]。 F_5 断裂带以成熟油为主,油气密度整体较高,呈现南低北高的特征,油气成熟度较高,南北差异相对较小; F_7 断裂带也以成熟油为主,原油密度

南低北高,成熟度表现出相同的变化规律; F_{16} 断裂带以高成熟凝析气为主,断裂内油气成熟度相对均一; F_{17} 以高成熟凝析气为主,断裂北部的油气密度较高,成熟度较低。统计分析表明,原油密度与气/油比和天然气干燥系数呈正相关关系,与黏度和胶质含量呈负相关关系,但干燥系数和胶质含量的相关性较弱,表明研究区油气藏经历了多期油气充注混合(图2a,b)。

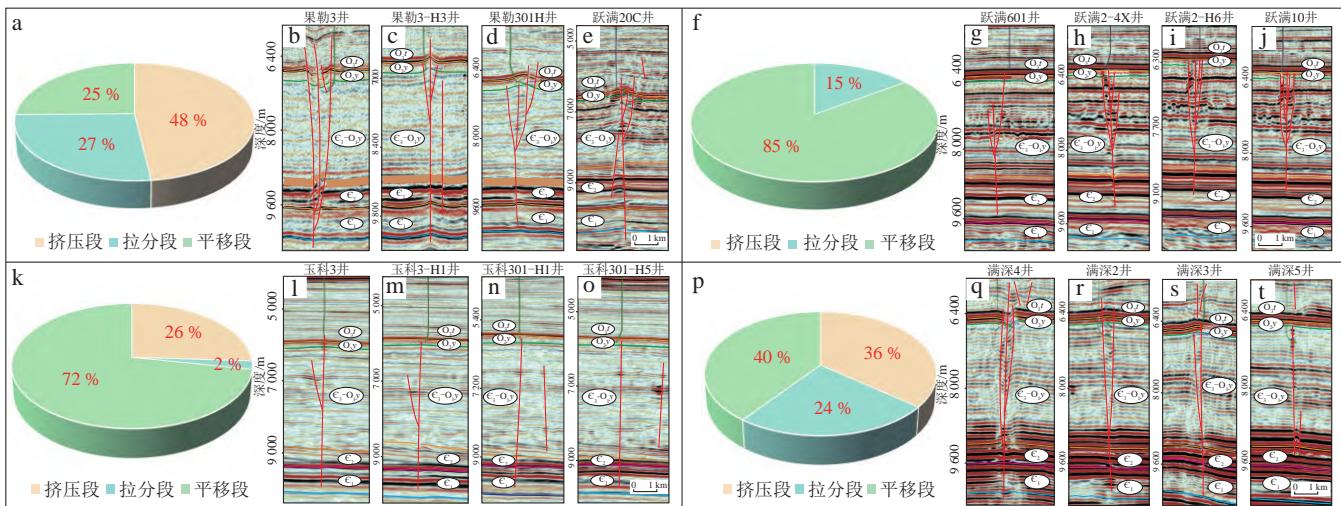


图3 富满地区典型走滑断裂带剖面几何结构特征

Fig. 3 Sections showing the geometric structures of typical strike-slip fault zones in the Fuman area

a. F₅断裂带不同应力段长度占比饼状图; b—e. F₅断裂带上各井垂直断裂带过井剖面; f. F₇断裂带应力段长度占比饼状图; g—j. F₇断裂带上各井垂直断裂带过井剖面; k. F₁₆断裂带应力段长度占比饼状图; l—o. F₁₆断裂带上各井垂直断裂带过井剖面; p. F₁₇断裂带应力段长度占比饼状图; q—t. F₁₇断裂带上各井垂直断裂带过井剖面

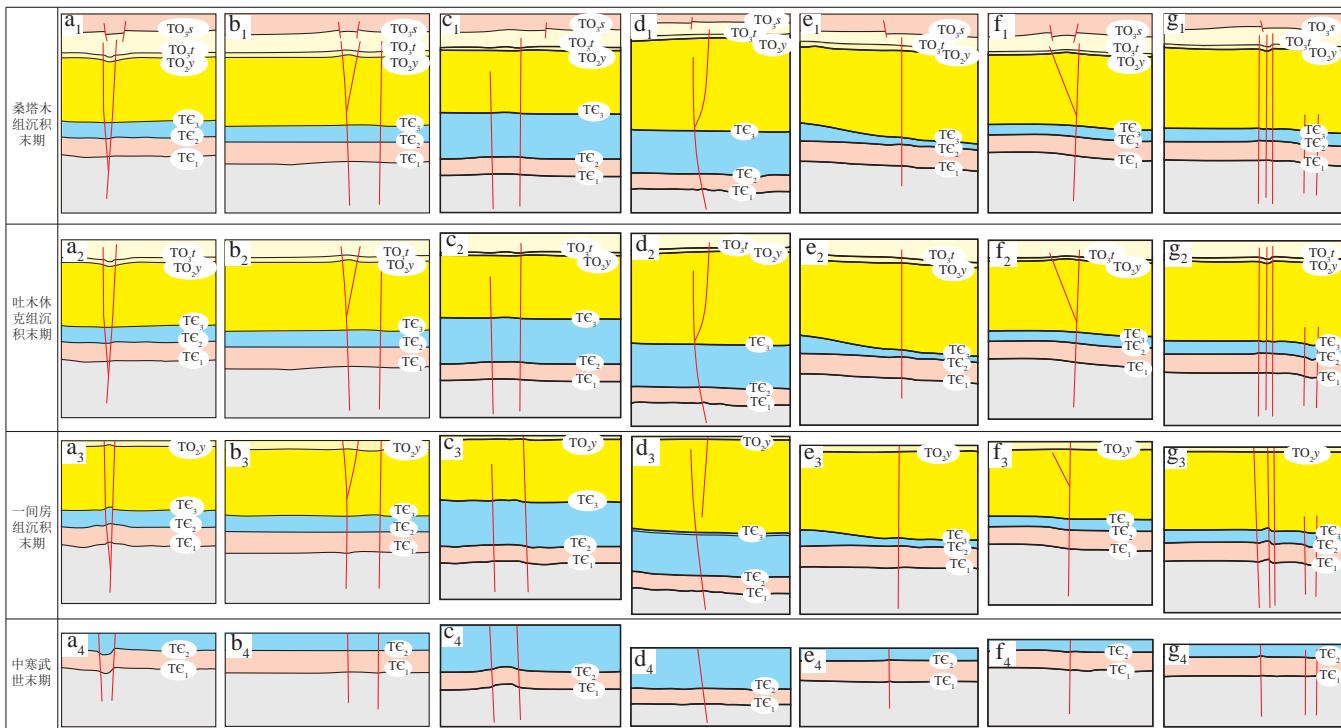


图4 富满地区典型断裂带构造演化过程

Fig. 4 Structural evolutionary processes of typical fault zones in the Fuman area

a₁—a₄, 果勒3井过井剖面, F₅断裂带; b₁—b₄, 果勒3-H3井过剖面, F₅断裂带; c₁—c₄, 跃满20-1X井过井剖面, F₅断裂带; d₁—d₄, 跃满5-1井过井剖面, F₇断裂带; e₁—e₄, 玉科302H井过井剖面, F₁₆断裂带; f₁—f₄, 满深3井过井剖面, F₁₇断裂带; g₁—g₄, 满深4井过井剖面, F₁₇断裂带

3.3 油气富集程度特征、变化规律及其差异

不同断裂带以及同一断裂带不同部位油气富集程度差异大(图6a—g), F₅断裂带油、水同产, F₁₇断裂带油、气、水同产, F₁₆断裂带以产气为主,由西向东,

油气产量呈递增的趋势。断裂带内部, F₅断裂带和 F₁₇断裂带油气产量整体呈北高南低的特征, 北部产水明显, F₇断裂带和 F₁₆断裂带南、北油气产量相对均匀, 产水量低。油气藏分布、油气性质及油气产出状态均与产量密切相关, 油气成熟度越低, 密度越高, 黏

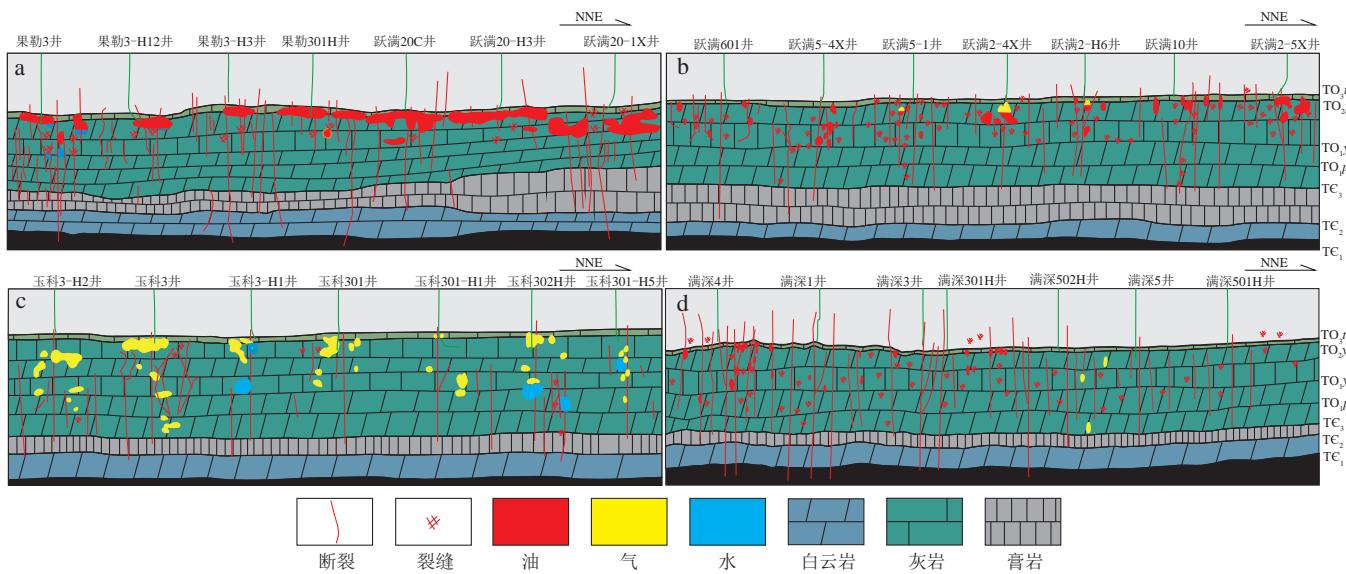


图5 富满地区典型走滑断裂带油藏剖面

Fig. 5 Oil reservoir profiles of typical strike-slip fault zones in the Fuman area

a. F₅断层带; b. F₇断层带; c. F₁₆断层带; d. F₁₇断层带

度越大,油气富集程度越低,油、气、水的分布规律越复杂,油气产量越低,油气藏规模越小。

4 走滑断裂差异演化控制下的油气成藏条件与成藏过程

4.1 走滑断裂通源性、输导性和储集性特征、配置及其差异

走滑断裂在超深层碳酸盐岩油气成藏中兼具沟通

烃源岩、输导油气和控制油气储集体特征的多重作用^[7, 9, 18, 25, 28, 31, 41],即通源性、输导性和储集性。其中,通源性指走滑断裂沟通玉尔吐斯组烃源岩的程度,输导性是指断裂对烃源岩与储层之间地层(主要为膏岩层)的贯穿程度,储集性主要指断控缝洞型储集体的储集空间大小和物性特征。

以断裂几何结构和样式分析为基础,通过纵向上断裂与烃源岩和膏岩地层的接触关系及其对目的层的改造程度,即目的层断面附近地层的变形程度(即目的层构造起伏高度与断裂带横向宽度的比值)计算,本文

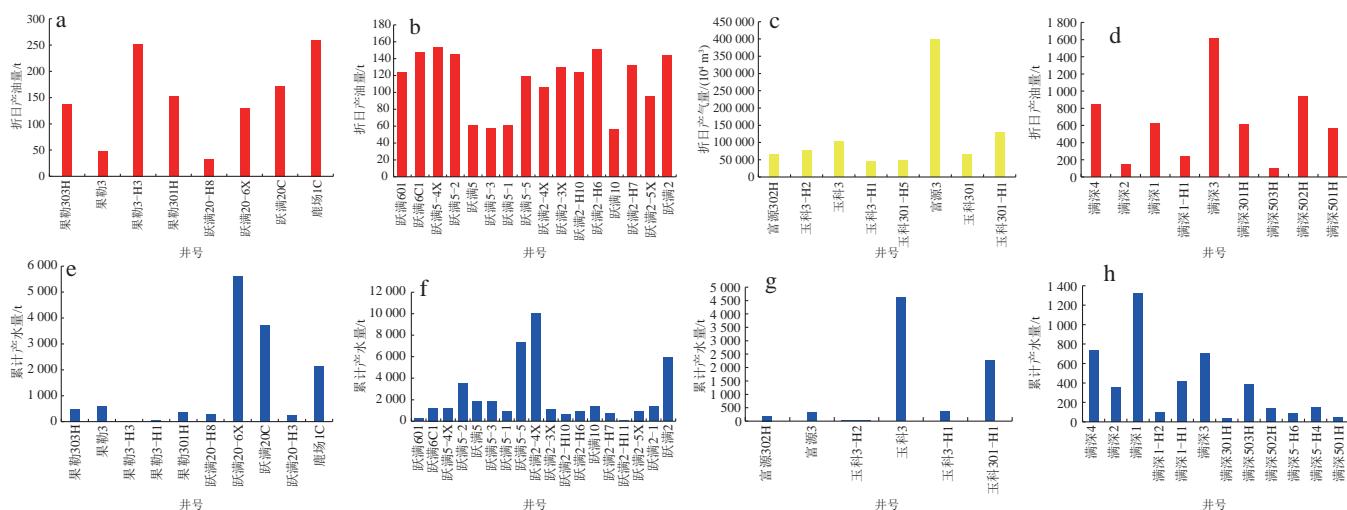


图6 富满地区典型断裂带油、气、水产量特征

Fig. 6 Histograms showing the oil, gas, and water yield of typical fault zones in the Fuman area

a—d. 各断裂带折日油、气产量柱状图; e—h. 各断裂带累计产水量柱状图

(a, e为F₅断层带; b, f为F₇断层带; c, g为F₁₆断层带; d, h为F₁₇断层带。)

提出了通源性和输导性的定量评价方法;基于钻井漏失量,结合地震能量体雕刻、岩心物性分析和微观孔隙空间发育特征,对断控储集体的储集性特征进行定量评价(图7)。

研究表明,走滑断裂通源性主要存在直接错断强通源型、未错断强通源型、未错断中通源型、未错断弱通源型和极弱通源型5种类型(表1)。挤压和拉分段以强、中通源型为主,平移段以弱通源型或极弱通源型为主,在应力叠接段,通源性普遍较好。受断裂差异演化的控制,断裂带间与断裂内通源性差异大,F₅断裂带整体通源,寒武系强烈弯曲或发生明显错断,形成了强挤压隆升、中通源的特征,存在少量弱通源部分,中部通源性强于两端(图8a);F₇断裂带寒武系稳定、平直、连续,未发生明显的弯曲或错断,通源性极差,在最南端的跃满601井显示出弱通源性,是油气的主要注入点(图8b);F₁₆断裂带在寒武系地震同相轴发生明显的弯曲,中通源型主要出现在挤压段,弱通源型主要出现在拉分段,中部较两端通源性更好(图8c);F₁₇断裂带通源性复杂,南部强通源,寒武系地震同相轴强烈弯曲、错断,北部弱通源或不通源,寒武系未发生明显错断或者强烈弯曲(图8d)。

输导性主要可以分为直接错断强输导型、未错断强输导型、未错断中输导型和未错断弱输导型4种类型(表1)。拉分段对膏岩层的改造作用更强,地层发生明显逃逸减薄,地震同相轴发生明显错断,输导性更强,挤压段和平移段则以中、弱输导为主。F₅断裂带以中输导为主,存在强输导,输导性差异较大(图8e);F₇断裂带以强、中输导为主,存在弱输导,差异较小(图8f);F₁₆断裂带整体以弱输导为主,输

导性较差(图8g);F₁₇断裂带输导性最强,直接错断强输导型占主导地位,断裂南部输导性强于北部(图8h)。

研究区奥陶系一间房组储集性存在优、中、差3种类型^[13, 34, 45, 54, 55]。优储集型以洞穴和孔洞为主,孔渗较高,微裂缝和溶蚀粒间孔发育,主要出现在拉分段和挤压段;中储集型洞穴的发育规模降低,孔洞和裂隙是主要的储集体,平均孔渗略有降低,微裂缝和溶蚀孔是主要的储集空间,主要出现在挤压段;差储集型孔洞、裂隙和基质孔隙共同构成了主要储集体,孔、渗较低,储集空间以基质孔隙为主,主要发育在平移段(表2)。

F₅断裂带和F₁₆断裂带以圆柱状和纺锤状的洞穴和孔洞为主体,缝洞体周缘的衍生断裂相互连接程度较弱,储集体相互连通程度较差;F₇断裂带和F₁₇断裂带沿断裂走向形成了洞穴、孔洞和裂隙组成的带状储集体,衍生裂隙带之间相互连通,沟通发育规模相对较小的洞穴和孔洞,为油气的侧向运移提供了有效通道(图9a—d)。

受到断裂差异演化的控制,不同断裂带的不同部位形成了不同通源性、输导性和储集性的成藏运聚条件配置关系(图10),其中,F₅断裂带配置关系差异大,发育强-中-中(强通源-中输导-中储集)(图10a)、弱-中-差、中-强-中(图10c)、中-中-差和弱-中-中配置关系(图10)。F₇断裂带和F₁₆断裂带的配置关系差异较小,F₇断裂带存在强-优(强输导-优储集)、强-中、中-差、弱-中和弱-差配置关系,F₁₆断裂带中主要存在中-强-差、中-弱-中(图10d)、弱-弱-中和弱-弱-差(图10e)配置关系,配置差异较小;F₁₇断裂带的配

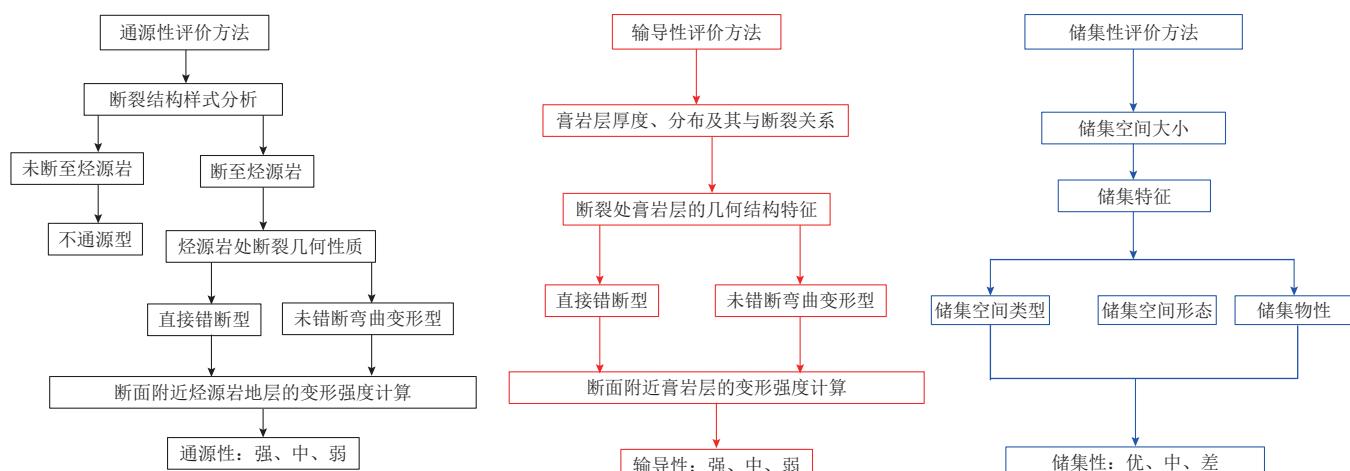


图7 走滑断裂带断控缝洞型油气藏运聚成藏条件综合评价流程与方法

Fig. 7 Flow chart and methods for the comprehensive assessment of hydrocarbon migration and accumulation conditions of fault-controlled fractured-vuggy hydrocarbon reservoirs in a strike-slip fault zone

表1 富满地区走滑断裂带通源性和输导性及其特征

Table 1 Characteristics of the connection to source rocks and hydrocarbon transport capacity of strike-slip fault zones in the Fuman area

		通源性		输导性			
类型		模式图	断裂附近地层 变形特征	变形强度	类型	模式图	断裂带附近地层 变形特征
强通 源型	直接错断强 通源型		地层直接错断,断距明显,地层平直,破碎程度高	>0.10	直接错断强 输导型 强输	<img alt="Geological model diagram for direct offset strong transport capacity. It shows a vertical red fault line intersecting green sedimentary layers labeled TO1_f, TO2_f, TO3_f, TO4_f, TO5_f, TO6_f, TO7_f, TO8_f, TO9_f, TO10_f, TO11_f, TO12_f, TO13_f, TO14_f, TO15_f, TO16_f, TO17_f, TO18_f, TO19_f, TO20_f, TO21_f, TO22_f, TO23_f, TO24_f, TO25_f, TO26_f, TO27_f, TO28_f, TO29_f, TO30_f, TO31_f, TO32_f, TO33_f, TO34_f, TO35_f, TO36_f, TO37_f, TO38_f, TO39_f, TO40_f, TO41_f, TO42_f, TO43_f, TO44_f, TO45_f, TO46_f, TO47_f, TO48_f, TO49_f, TO50_f, TO51_f, TO52_f, TO53_f, TO54_f, TO55_f, TO56_f, TO57_f, TO58_f, TO59_f, TO60_f, TO61_f, TO62_f, TO63_f, TO64_f, TO65_f, TO66_f, TO67_f, TO68_f, TO69_f, TO70_f, TO71_f, TO72_f, TO73_f, TO74_f, TO75_f, TO76_f, TO77_f, TO78_f, TO79_f, TO80_f, TO81_f, TO82_f, TO83_f, TO84_f, TO85_f, TO86_f, TO87_f, TO88_f, TO89_f, TO90_f, TO91_f, TO92_f, TO93_f, TO94_f, TO95_f, TO96_f, TO97_f, TO98_f, TO99_f, TO100_f, TO101_f, TO102_f, TO103_f, TO104_f, TO105_f, TO106_f, TO107_f, TO108_f, TO109_f, TO110_f, TO111_f, TO112_f, TO113_f, TO114_f, TO115_f, TO116_f, TO117_f, TO118_f, TO119_f, TO120_f, TO121_f, TO122_f, TO123_f, TO124_f, TO125_f, TO126_f, TO127_f, TO128_f, TO129_f, TO130_f, TO131_f, TO132_f, TO133_f, TO134_f, TO135_f, TO136_f, TO137_f, TO138_f, TO139_f, TO140_f, TO141_f, TO142_f, TO143_f, TO144_f, TO145_f, TO146_f, TO147_f, TO148_f, TO149_f, TO150_f, TO151_f, TO152_f, TO153_f, TO154_f, TO155_f, TO156_f, TO157_f, TO158_f, TO159_f, TO160_f, TO161_f, TO162_f, TO163_f, TO164_f, TO165_f, TO166_f, TO167_f, TO168_f, TO169_f, TO170_f, TO171_f, TO172_f, TO173_f, TO174_f, TO175_f, TO176_f, TO177_f, TO178_f, TO179_f, TO180_f, TO181_f, TO182_f, TO183_f, TO184_f, TO185_f, TO186_f, TO187_f, TO188_f, TO189_f, TO190_f, TO191_f, TO192_f, TO193_f, TO194_f, TO195_f, TO196_f, TO197_f, TO198_f, TO199_f, TO200_f, TO201_f, TO202_f, TO203_f, TO204_f, TO205_f, TO206_f, TO207_f, TO208_f, TO209_f, TO210_f, TO211_f, TO212_f, TO213_f, TO214_f, TO215_f, TO216_f, TO217_f, TO218_f, TO219_f, TO220_f, TO221_f, TO222_f, TO223_f, TO224_f, TO225_f, TO226_f, TO227_f, TO228_f, TO229_f, TO230_f, TO231_f, TO232_f, TO233_f, TO234_f, TO235_f, TO236_f, TO237_f, TO238_f, TO239_f, TO240_f, TO241_f, TO242_f, TO243_f, TO244_f, TO245_f, TO246_f, TO247_f, TO248_f, TO249_f, TO250_f, TO251_f, TO252_f, TO253_f, TO254_f, TO255_f, TO256_f, TO257_f, TO258_f, TO259_f, TO260_f, TO261_f, TO262_f, TO263_f, TO264_f, TO265_f, TO266_f, TO267_f, TO268_f, TO269_f, TO270_f, TO271_f, TO272_f, TO273_f, TO274_f, TO275_f, TO276_f, TO277_f, TO278_f, TO279_f, TO280_f, TO281_f, TO282_f, TO283_f, TO284_f, TO285_f, TO286_f, TO287_f, TO288_f, TO289_f, TO290_f, TO291_f, TO292_f, TO293_f, TO294_f, TO295_f, TO296_f, TO297_f, TO298_f, TO299_f, TO300_f, TO310_f, TO320_f, TO330_f, TO340_f, TO350_f, TO360_f, TO370_f, TO380_f, TO390_f, TO400_f, TO410_f, TO420_f, TO430_f, TO440_f, TO450_f, TO460_f, TO470_f, TO480_f, TO490_f, TO500_f, TO510_f, TO520_f, TO530_f, TO540_f, TO550_f, TO560_f, TO570_f, TO580_f, TO590_f, TO600_f, TO610_f, TO620_f, TO630_f, TO640_f, TO650_f, TO660_f, TO670_f, TO680_f, TO690_f, TO700_f, TO710_f, TO720_f, TO730_f, TO740_f, TO750_f, TO760_f, TO770_f, TO780_f, TO790_f, TO800_f, TO810_f, TO820_f, TO830_f, TO840_f, TO850_f, TO860_f, TO870_f, TO880_f, TO890_f, TO900_f, TO910_f, TO920_f, TO930_f, TO940_f, TO950_f, TO960_f, TO970_f, TO980_f, TO990_f, TO1000_f, TO1010_f, TO1020_f, TO1030_f, TO1040_f, TO1050_f, TO1060_f, TO1070_f, TO1080_f, TO1090_f, TO1100_f, TO1110_f, TO1120_f, TO1130_f, TO1140_f, TO1150_f, TO1160_f, TO1170_f, TO1180_f, TO1190_f, TO1200_f, TO1210_f, TO1220_f, TO1230_f, TO1240_f, TO1250_f, TO1260_f, TO1270_f, TO1280_f, TO1290_f, TO1300_f, TO1310_f, TO1320_f, TO1330_f, TO1340_f, TO1350_f, TO1360_f, TO1370_f, TO1380_f, TO1390_f, TO1400_f, TO1410_f, TO1420_f, TO1430_f, TO1440_f, TO1450_f, TO1460_f, TO1470_f, TO1480_f, TO1490_f, TO1500_f, TO1510_f, TO1520_f, TO1530_f, TO1540_f, TO1550_f, TO1560_f, TO1570_f, TO1580_f, TO1590_f, TO1600_f, TO1610_f, TO1620_f, TO1630_f, TO1640_f, TO1650_f, TO1660_f, TO1670_f, TO1680_f, TO1690_f, TO1700_f, TO1710_f, TO1720_f, TO1730_f, TO1740_f, TO1750_f, TO1760_f, TO1770_f, TO1780_f, TO1790_f, TO1800_f, TO1810_f, TO1820_f, TO1830_f, TO1840_f, TO1850_f, TO1860_f, TO1870_f, TO1880_f, TO1890_f, TO1900_f, TO1910_f, TO1920_f, TO1930_f, TO1940_f, TO1950_f, TO1960_f, TO1970_f, TO1980_f, TO1990_f, TO2000_f, TO2010_f, TO2020_f, TO2030_f, TO2040_f, TO2050_f, TO2060_f, TO2070_f, TO2080_f, TO2090_f, TO2100_f, TO2110_f, TO2120_f, TO2130_f, TO2140_f, TO2150_f, TO2160_f, TO2170_f, TO2180_f, TO2190_f, TO2200_f, TO2210_f, TO2220_f, TO2230_f, TO2240_f, TO2250_f, TO2260_f, TO2270_f, TO2280_f, TO2290_f, TO2300_f, TO2310_f, TO2320_f, TO2330_f, TO2340_f, TO2350_f, TO2360_f, TO2370_f, TO2380_f, TO2390_f, TO2400_f, TO2410_f, TO2420_f, TO2430_f, TO2440_f, TO2450_f, TO2460_f, TO2470_f, TO2480_f, TO2490_f, TO2500_f, TO2510_f, TO2520_f, TO2530_f, TO2540_f, TO2550_f, TO2560_f, TO2570_f, TO2580_f, TO2590_f, TO2600_f, TO2610_f, TO2620_f, TO2630_f, TO2640_f, TO2650_f, TO2660_f, TO2670_f, TO2680_f, TO2690_f, TO2700_f, TO2710_f, TO2720_f, TO2730_f, TO2740_f, TO2750_f, TO2760_f, TO2770_f, TO2780_f, TO2790_f, TO2800_f, TO2810_f, TO2820_f, TO2830_f, TO2840_f, TO2850_f, TO2860_f, TO2870_f, TO2880_f, TO2890_f, TO2900_f, TO2910_f, TO2920_f, TO2930_f, TO2940_f, TO2950_f, TO2960_f, TO2970_f, TO2980_f, TO2990_f, TO3000_f, TO3100_f, TO3200_f, TO3300_f, TO3400_f, TO3500_f, TO3600_f, TO3700_f, TO3800_f, TO3900_f, TO4000_f, TO4100_f, TO4200_f, TO4300_f, TO4400_f, TO4500_f, TO4600_f, TO4700_f, TO4800_f, TO4900_f, TO5000_f, TO5100_f, TO5200_f, TO5300_f, TO5400_f, TO5500_f, TO5600_f, TO5700_f, TO5800_f, TO5900_f, TO6000_f, TO6100_f, TO6200_f, TO6300_f, TO6400_f, TO6500_f, TO6600_f, TO6700_f, TO6800_f, TO6900_f, TO7000_f, TO7100_f, TO7200_f, TO7300_f, TO7400_f, TO7500_f, TO7600_f, TO7700_f, TO7800_f, TO7900_f, TO8000_f, TO8100_f, TO8200_f, TO8300_f, TO8400_f, TO8500_f, TO8600_f, TO8700_f, TO8800_f, TO8900_f, TO9000_f, TO9100_f, TO9200_f, TO9300_f, TO9400_f, TO9500_f, TO9600_f, TO9700_f, TO9800_f, TO9900_f, TO10000_f, TO10100_f, TO10200_f, TO10300_f, TO10400_f, TO10500_f, TO10600_f, TO10700_f, TO10800_f, TO10900_f, TO11000_f, TO11100_f, TO11200_f, TO11300_f, TO11400_f, TO11500_f, TO11600_f, TO11700_f, TO11800_f, TO11900_f, TO12000_f, TO12100_f, TO12200_f, TO12300_f, TO12400_f, TO12500_f, TO12600_f, TO12700_f, TO12800_f, TO12900_f, TO13000_f, TO13100_f, TO13200_f, TO13300_f, TO13400_f, TO13500_f, TO13600_f, TO13700_f, TO13800_f, TO13900_f, TO14000_f, TO14100_f, TO14200_f, TO14300_f, TO14400_f, TO14500_f, TO14600_f, TO14700_f, TO14800_f, TO14900_f, TO15000_f, TO15100_f, TO15200_f, TO15300_f, TO15400_f, TO15500_f, TO15600_f, TO15700_f, TO15800_f, TO15900_f, TO16000_f, TO16100_f, TO16200_f, TO16300_f, TO16400_f, TO16500_f, TO16600_f, TO16700_f, TO16800_f, TO16900_f, TO17000_f, TO17100_f, TO17200_f, TO17300_f, TO17400_f, TO17500_f, TO17600_f, TO17700_f, TO17800_f, TO17900_f, TO18000_f, TO18100_f, TO18200_f, TO18300_f, TO18400_f, TO18500_f, TO18600_f, TO18700_f, TO18800_f, TO18900_f, TO19000_f, TO19100_f, TO19200_f, TO19300_f, TO19400_f, TO19500_f, TO19600_f, TO19700_f, TO19800_f, TO19900_f, TO20000_f, TO20100_f, TO20200_f, TO20300_f, TO20400_f, TO20500_f, TO20600_f, TO20700_f, TO20800_f, TO20900_f, TO21000_f, TO21100_f, TO21200_f, TO21300_f, TO21400_f, TO21500_f, TO21600_f, TO21700_f, TO21800_f, TO21900_f, TO22000_f, TO22100_f, TO22200_f, TO22300_f, TO22400_f, TO22500_f, TO22600_f, TO22700_f, TO22800_f, TO22900_f, TO23000_f, TO23100_f, TO23200_f, TO23300_f, TO23400_f, TO23500_f, TO23600_f, TO23700_f, TO23800_f, TO23900_f, TO24000_f, TO24100_f, TO24200_f, TO24300_f, TO24400_f, TO24500_f, TO24600_f, TO24700_f, TO24800_f, TO24900_f, TO25000_f, TO25100_f, TO25200_f, TO25300_f, TO25400_f, TO25500_f, TO25600_f, TO25700_f, TO25800_f, TO25900_f, TO26000_f, TO26100_f, TO26200_f, TO26300_f, TO26400_f, TO26500_f, TO26600_f, TO26700_f, TO26800_f, TO26900_f, TO27000_f, TO27100_f, TO27200_f, TO27300_f, TO27400_f, TO27500_f, TO27600_f, TO27700_f, TO27800_f, TO27900_f, TO28000_f, TO28100_f, TO28200_f, TO28300_f, TO28400_f, TO28500_f, TO28600_f, TO28700_f, TO28800_f, TO28900_f, TO29000_f, TO29100_f, TO29200_f, TO29300_f, TO29400_f, TO29500_f, TO29600_f, TO29700_f, TO29800_f, TO29900_f, TO30000_f, TO31000_f, TO32000_f, TO33000_f, TO34000_f, TO35000_f, TO36000_f, TO37000_f, TO38000_f, TO39000_f, TO40000_f, TO41000_f, TO42000_f, TO43000_f, TO44000_f, TO45000_f, TO46000_f, TO47000_f, TO48000_f, TO49000_f, TO50000_f, TO51000_f, TO52000_f, TO53000_f, TO54000_f, TO55000_f, TO56000_f, TO57000_f, TO58000_f, TO59000_f, TO60000_f, TO61000_f, TO62000_f, TO63000_f, TO64000_f, TO65000_f, TO66000_f, TO67000_f, TO68000_f, TO69000_f, TO70000_f, TO71000_f, TO72000_f, TO73000_f, TO74000_f, TO75000_f, TO76000_f, TO77000_f, TO78000_f, TO79000_f, TO80000_f, TO81000_f, TO82000_f, TO83000_f, TO84000_f, TO85000_f, TO86000_f, TO87000_f, TO88000_f, TO89000_f, TO90000_f, TO91000_f, TO92000_f, TO93000_f, TO94000_f, TO95000_f, TO96000_f, TO97000_f, TO98000_f, TO99000_f, TO100000_f, TO101000_f, TO102000_f, TO103000_f, TO104000_f, TO105000_f, TO106000_f, TO107000_f, TO108000_f, TO109000_f, TO110000_f, TO111000_f, TO112000_f, TO113000_f, TO114000_f, TO115000_f, TO116000_f, TO117000_f, TO118000_f, TO119000_f, TO120000_f, TO121000_f, TO122000_f, TO123000_f, TO124000_f, TO125000_f, TO126000_f, TO127000_f, TO128000_f, TO129000_f, TO130000_f, TO131000_f, TO132000_f, TO133000_f, TO134000_f, TO135000_f, TO136000_f, TO137000_f, TO138000_f, TO139000_f, TO140000_f, TO141000_f, TO142000_f, TO143000_f, TO144000_f, TO145000_f, TO146000_f, TO147000_f, TO148000_f, TO149000_f, TO150000_f, TO151000_f, TO152000_f, TO153000_f, TO154000_f, TO155000_f, TO156000_f, TO157000_f, TO158000_f, TO159000_f, TO160000_f, TO161000_f, TO162000_f, TO163000_f, TO164000_f, TO165000_f, TO166000_f, TO167000_f, TO168000_f, TO169000_f, TO170000_f, TO171000_f, TO172000_f, TO173000_f, TO174000_f, TO175000_f, TO176000_f, TO177000_f, TO178000_f, TO179000_f, TO180000_f, TO181000_f, TO182000_f, TO183000_f, TO184000_f, TO185000_f, TO186000_f, TO187000_f, TO188000_f, TO189000_f, TO190000_f, TO191000_f, TO192000_f, TO193000_f, TO194000_f, TO195000_f, TO196000_f, TO197000_f, TO198000_f, TO199000_f, TO200000_f, TO201000_f, TO202000_f, TO203000_f, TO204000_f, TO205000_f, TO206000_f, TO207000_f, TO208000_f, TO209000_f, TO210000_f, TO211000_f, TO212000_f, TO213000_f, TO214000_f, TO215000_f, TO216000_f, TO217000_f, TO218000_f, TO219000_f, TO220000_f, TO221000_f, TO222000_f, TO223000_f, TO224000_f, TO225000_f, TO226000_f, TO227000_f, TO228000_f, TO229000_f, TO230000_f, TO231000_f, TO232000_f, TO233000_f, TO234000_f, TO235000_f, TO236000_f, TO237000_f, TO238000_f, TO239000_f, TO240000_f, TO241000_f, TO242000_f, TO243000_f, TO244000_f, TO245000_f, TO246000_f, TO247000_f, TO248000_f, TO249000_f, TO250000_f, TO251000_f, TO252000_f, TO253000_f, TO254000_f, TO255000_f, TO256000_f, TO257000_f, TO258000_f, TO259000_f, TO260000_f, TO261000_f, TO262000_f, TO263000_f, TO264000_f, TO265000_f, TO266000_f, TO267000_f, TO268000_f, TO269000_f, TO270000_f, TO271000_f, TO272000_f, TO273000_f, TO274000_f, TO275000_f, TO276000_f, TO277000_f, TO278000_f, TO279000_f, TO280000_f, TO281000_f, TO282000_f, TO283000_f, TO284000_f, TO285000_f, TO286000_f, TO287000_f, TO288000_f, TO289000_f, TO290000_f, TO291000_f, TO292000_f, TO293000_f, TO294000_f, TO295000_f, TO296000_f, TO297000_f, TO298000_f, TO299000_f, TO300000_f, TO310000_f, TO320000_f, TO330000_f, TO340000_f, TO350000_f, TO360000_f, TO370000_f, TO380000_f, TO390000_f, TO400000_f, TO410000_f, TO420000_f, TO430000_f, TO440000_f, TO450000_f, TO460000_f, TO470000_f, TO480000_f, TO490000_f, TO500000_f, TO510000_f, TO520000_f, TO530000_f, TO540000_f, TO550000_f, TO560000_f, TO570000_f, TO580000_f, TO590000_f, TO600000_f, TO610000_f, TO620000_f, TO630000_f, TO640000_f, TO650000_f, TO660000_f, TO670000_f, TO680000_f, TO690000_f, TO700000_f, TO710000_f, TO720000_f, TO730000_f, TO740000_f, TO750000_f, TO760000_f, TO770000_f, TO780000_f, TO790000_f, TO800000_f, TO810000_f, TO820000_f, TO830000_f, TO840000_f, TO850000_f, TO860000_f, TO870000_f, TO880000_f, TO890000_f, TO900000_f, TO910000_f, TO920000_f, TO930000_f, TO940000_f, TO950000_f, TO960000_f, TO970000_f, TO980000_f, TO990000_f, TO1000000_f, TO1010000_f, TO1020000_f, TO1030000_f, TO1040000_f, TO1050000_f, TO1060000_f, TO1070000_f, TO1080000_f, TO1090000_f, TO1100000_f, TO1110000_f, TO1120000_f, TO1130000_f, TO1140000_f, TO1150000_f, TO1160000_f, TO1170000_f, TO1180000_f, TO1190000_f, TO1200000_f, TO1210000_f, TO1220000_f, TO1230000_f, TO1240000_f, TO1250000_f, TO1260000_f, TO1270000_f, TO1280000_f, TO1290000_f, TO1300000_f, TO1310000_f, TO1320000_f, TO1330000_f, TO1340000_f, TO1350000_f, TO1360000_f, TO1370000_f, TO1380000_f, TO1390000_f, TO1400000_f, TO1410000_f, TO1420000_f, TO1430000_f, TO1440000_f, TO1450000_f, TO1460000_f, TO1470000_f, TO1480000_f, TO1490000_f, TO1500000_f, TO1510000_f, TO1520000_f, TO1530000_f, TO1540000_f, TO1550000_f, TO1560000_f, TO1570000_f, TO1580000_f, TO1590000_f, TO1600000_f, TO1610000_f, TO1620000_f, TO1630000_f, TO1640000_f, TO1650000_f, TO1660000_f, TO1670000_f, TO1680000_f, TO1690000_f, TO1700000_f, TO1710000_f, TO1720000_f, TO1730000_f, TO1740000_f, TO1750000_f, TO1760000_f, TO1770000_f, TO1780000_f, TO1790000_f, TO1800000_f, TO1810000_f, TO1820000_f, TO1830000_f, TO1840000_f, TO1850000_f, TO1860000_f, TO1870000_f, TO1880000_f, TO1890000_f, TO1900000_f, TO1910000_f, TO1920000_f, TO1930000_f, TO1940000_f, TO1950000_f, TO1960000_f, TO1970000_f, TO1980000_f, TO1990000_f, TO2000000_f, TO2010000_f, TO2020000_f, TO2030000_f, TO2040000_f, TO2050000_f, TO2060000_f, TO2070000_f, TO2080000_f, TO2090000_f, TO2100000_f, TO2110000_f, TO2120000_f, TO2130000_f, TO2140000_f, TO2150000_f, TO2160000_f, TO2170000_f, TO2180000_f, TO2190000_f, TO2200000_f, TO2210000_f, TO2220000_f, TO2230000_f, TO2240000_f, TO2250000_f, TO2260000_f, TO2270000_f, TO2280000_f, TO2290000_f, TO2300000_f, TO2310000_f, TO2320000_f, TO2330000_f, TO2340000_f, TO2350000_f, TO2360000_f, TO2370000_f, TO2380000_f, TO2390000_f, TO2400000_f, TO2410000_f, TO2420000_f, TO2430000_f, TO2440000_f, TO2450000_f, TO2460000_f, TO2470000_f, TO2480000_f, TO2490000_f, TO2500000_f, TO2510000_f, TO2520000_f, TO2530000_f, TO2540000_f, TO2550000_f, TO2560000_f, TO2570000_f, TO2580000_f, TO2590000_f, TO2600000_f, TO2610000_f, TO2620000_f, TO2630000_f, TO2640000_f, TO2650000_f, TO2660000_f, TO2670000_f, TO2680000_f, TO2690000_f, TO27	

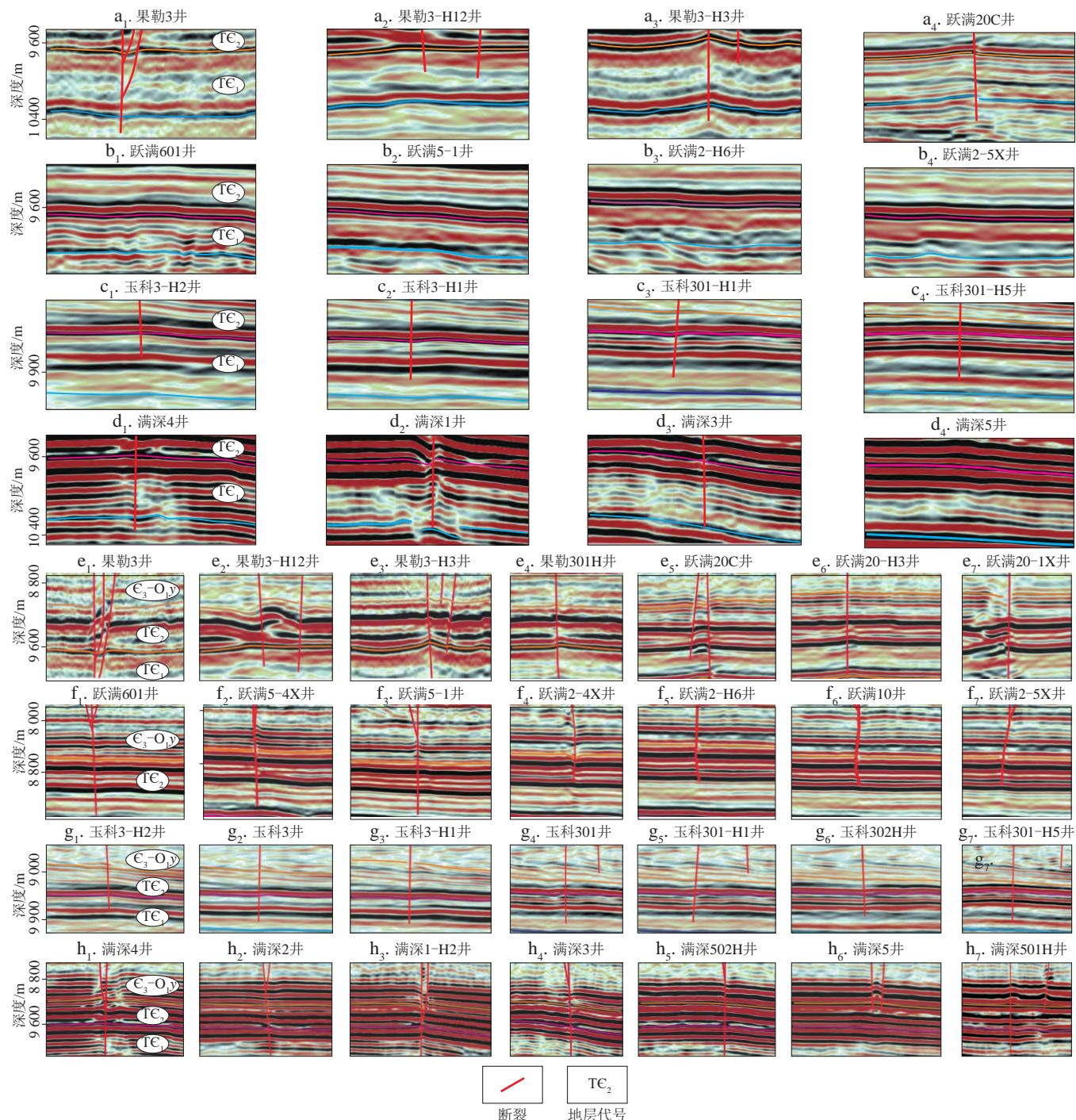


图8 富满地区典型断裂带通源性和输导性特征及其差异

Fig. 8 Differences in the connection to source rocks and hydrocarbon transport capacities of typical strike-slip fault zones in the Fuman area
 a_1-a_4 . F_{15} 断裂带通源性特征; b_1-b_4 , F_{17} 断裂带通源性特征; c_1-c_4 , F_{16} 断裂带通源性特征; d_1-d_4 , F_{17} 断裂带通源性特征; e_1-e_7 , F_{15} 断裂带
 输导性特征; f_1-f_7 , F_{17} 断裂带输导性特征; g_1-g_7 , F_{16} 断裂带输导性特征; h_1-h_7 , F_{17} 断裂带输导性特征

置关系相对均一,发育强-强-优(图10b)和强-强-中2种类型,该断裂多期活动性都较强,发育相对均一且较好的配置关系。

4.2 走滑断裂演化控制下的油气充注期次及其差异

富满地区主要经历了加里东晚期、海西晚期和喜

马拉雅期3期油气充注^[19, 40, 56-57],在不同断裂间及同一断裂内油气充注期次存在明显区别,主要受到断裂演化与烃源岩热演化过程及生、排烃期次时-空耦合关系的控制。研究区玉尔吐斯组烃源岩从中、晚寒武纪开始持续生、排烃,油气充注发生在断裂强活动期,断裂演化过程的差异导致油气充注期次差异。这种差异

表2 富满地区奥陶系一间房组碳酸盐储层储集性能评价

Table 2 Evaluation of the storage capacity of carbonate reservoirs in the Ordovician Yijianfang Formation, Fuman area

储集性能	优储集	中储集	差储集																														
储集模式示意图																																	
储集系数	>1.5	0.5~1.5	<0.5																														
储集空间类型	分支断裂发育,断裂面附近发育规模性的洞穴,向周缘发育宽度较大的缝洞发育带和衍生裂缝带,洞穴和孔洞是主要储集空间	分支断裂较发育,仅在主干断裂面附近发育较小规模的洞穴,周缘缝洞发育带规模减小,发育较大规模的衍生裂缝带,洞穴、孔洞和裂缝是主要储集空间	分支断裂不发育,洞穴不发育,周缘缝洞发育带规模较小,发育较大规模的衍生裂缝带,孔洞、裂缝及基质孔隙是主要储集空间																														
储集空间形态	球形、纺锤形、条形	以球形为主	以条形或者纺锤形为主																														
储集物性特征	<table border="1"> <caption>Data from F17 fracture zone chart</caption> <thead> <tr> <th>井号</th> <th>岩心 (%)</th> <th>岩心裂缝 (%)</th> </tr> </thead> <tbody> <tr> <td>跃满2</td> <td>1.10</td> <td>0.75</td> </tr> <tr> <td>跃满5</td> <td>0.97</td> <td>1.03</td> </tr> <tr> <td>跃满6</td> <td>2.01</td> <td>-</td> </tr> </tbody> </table>	井号	岩心 (%)	岩心裂缝 (%)	跃满2	1.10	0.75	跃满5	0.97	1.03	跃满6	2.01	-	<table border="1"> <caption>Data from F17 fracture zone chart</caption> <thead> <tr> <th>井号</th> <th>岩心 (%)</th> <th>岩心裂缝 (%)</th> </tr> </thead> <tbody> <tr> <td>哈得32</td> <td>0.45</td> <td>2.55</td> </tr> <tr> <td>满深2</td> <td>1.15</td> <td>0.65</td> </tr> </tbody> </table>	井号	岩心 (%)	岩心裂缝 (%)	哈得32	0.45	2.55	满深2	1.15	0.65	<table border="1"> <caption>Data from F15 fracture zone chart</caption> <thead> <tr> <th>物性</th> <th>岩心 (%)</th> <th>渗透率 (10^-3 μm^2)</th> </tr> </thead> <tbody> <tr> <td>孔隙度</td> <td>0.65</td> <td>-</td> </tr> <tr> <td>渗透率</td> <td>-</td> <td>35</td> </tr> </tbody> </table>	物性	岩心 (%)	渗透率 (10^-3 μm^2)	孔隙度	0.65	-	渗透率	-	35
井号	岩心 (%)	岩心裂缝 (%)																															
跃满2	1.10	0.75																															
跃满5	0.97	1.03																															
跃满6	2.01	-																															
井号	岩心 (%)	岩心裂缝 (%)																															
哈得32	0.45	2.55																															
满深2	1.15	0.65																															
物性	岩心 (%)	渗透率 (10^-3 μm^2)																															
孔隙度	0.65	-																															
渗透率	-	35																															
微观储集空间特征																																	
发育应力段	拉分段为主,挤压段次之	挤压段为主,平移段次之	主要出现在平移段,少量出现在挤压段																														

在F5断裂带最为明显:断裂带南部多期持续活动,流体包裹体均一温度数据指示南部发生了2~3期油气充注,油气成熟度高、密度低;断裂带北部早期活动、晚期定型,油藏以早、中期原油充注为主,油气成熟度低(图11a—d)。断裂整体强持续活动的F16断裂带和F17断裂带,烃源岩热演化程度高,晚期生成的高成熟天然气大量充注,整体油气成熟度高,气洗作用明显

(图11a)。F7断裂带北部通源性很差,油气等效镜质体反射率由南向北递减,原油中轻质组分减少,表现出侧向运移的特征。按油气生成和充注顺序,早期生成的原油先运移至北部高部位,后期生成的油气主要在南部低部位的充注点附近(图11a,e—g)。流体包裹体均一温度指示了相同的变化规律,靠近充注点的断裂带南部,存在3期油气充注,向北部,油气充注期次逐

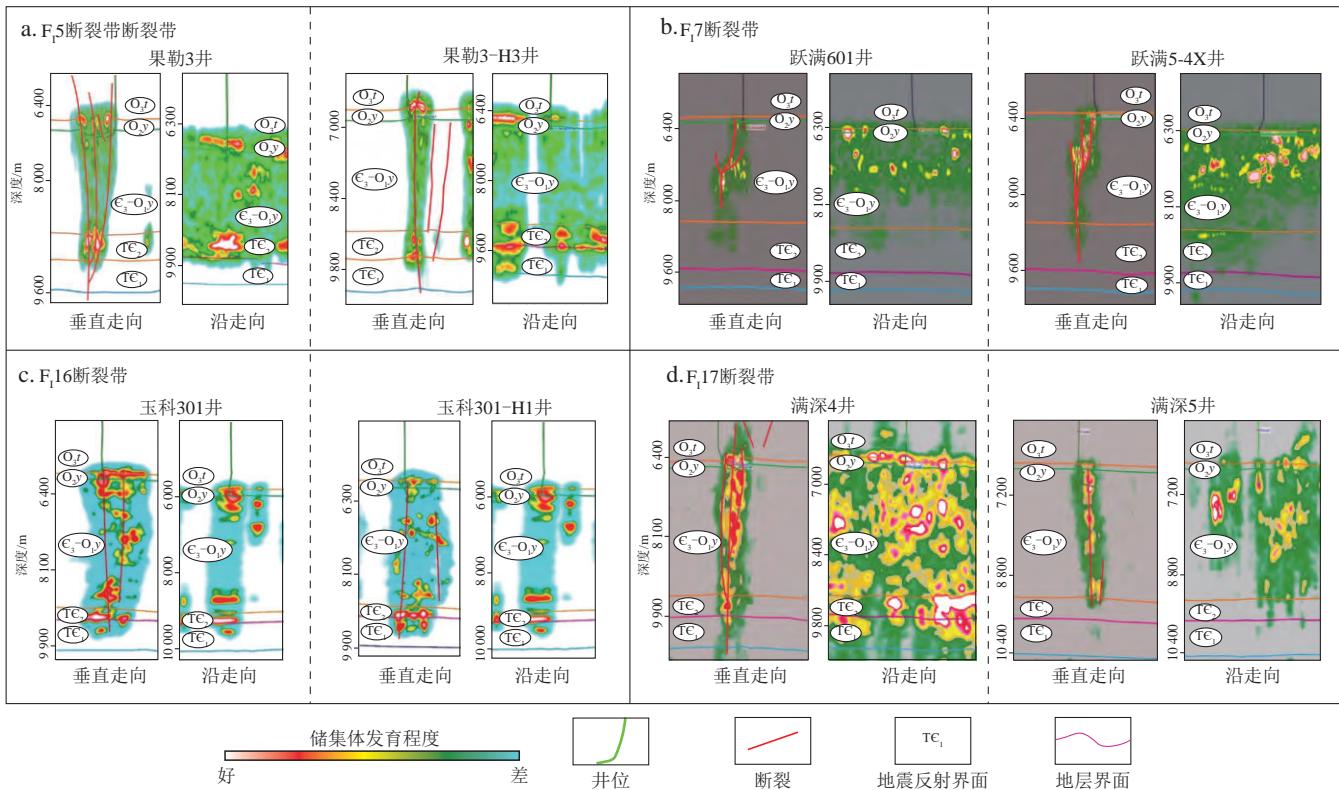


图9 富满地区典型走滑断裂带储层空间分布特征

Fig. 9 Spatial distribution of reservoirs in typical strike-slip fault zones in the Fuman area

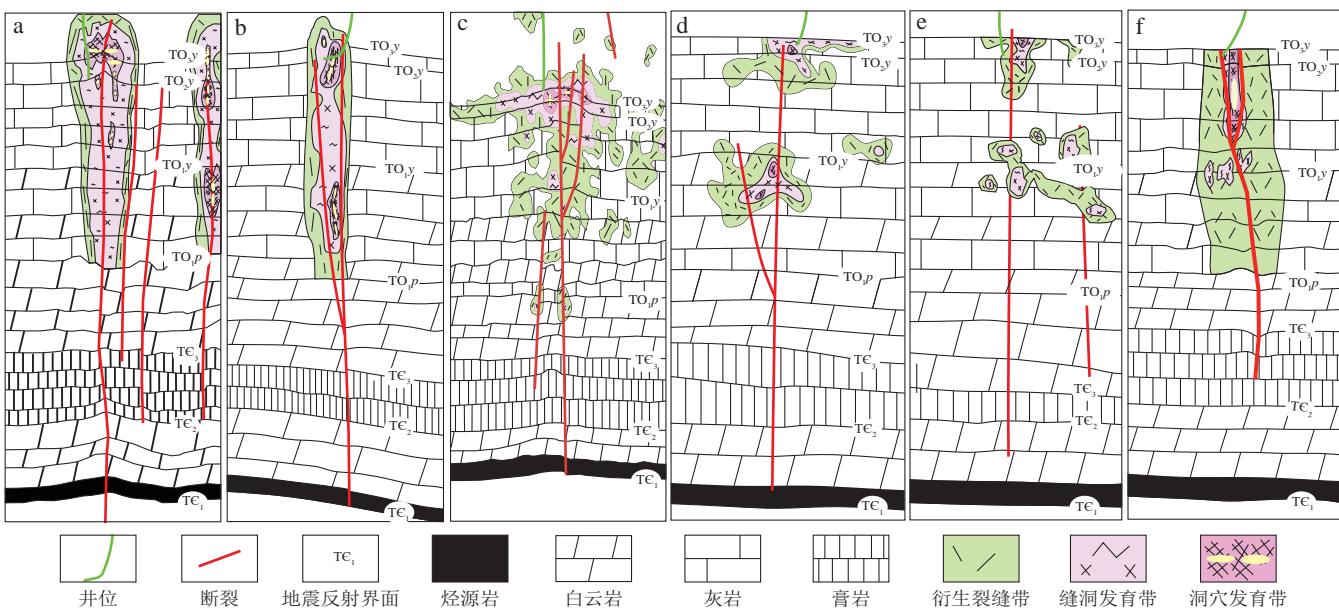


图10 富满地区走滑断裂带油气运聚成藏条件耦合配置关系示意图

Fig. 10 Schematic diagrams showing the coupling of hydrocarbon migration and accumulation conditions in the strike-slip fault zones in the Fuman area

a. 强通源-中输导-中储集型; b. 强通源-强输导-优储集型; c. 中通源-强输导-中储集型; d. 中通源-弱输导-中储集型; e. 弱通源-弱输导-差储集型; f. 极弱通源-强输导-优储集型

渐减少至2期,在最北端仅存在早期的1期油气充注,考虑到F₇断裂带在北部较差的通源性和带状储集体

的连通性,认为断裂带北段很大程度上存在侧向运移(图8b;图9b;图11a,e—g)。

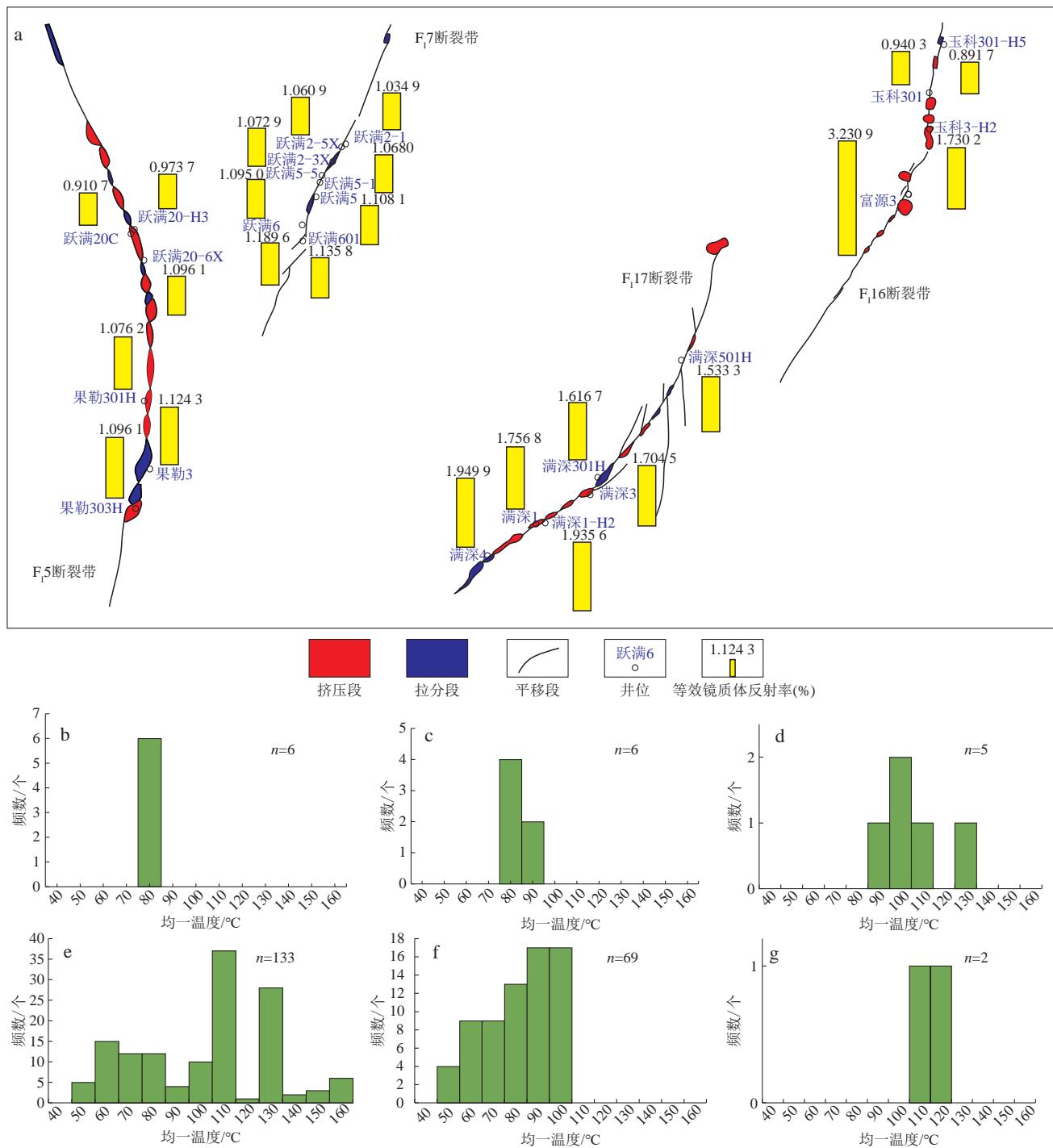


图11 富满地区走滑断裂带油气充注期次及其差异

Fig. 11 Hydrocarbon charging stages and their differences in the Fuman area

a. 典型走滑断裂带油气成熟度平面分布变化；b-d. F₅断裂带顺断裂走向流体包裹体均一温度频数分布直方图，分别对应断裂带南部、中部和北部；e—g F₇断裂带顺断裂走向流体包裹体均一温度频数分布直方图，分别对应断裂带南部、中部和北部

4.3 油气充注模式

通过综合分析富满地区走滑断裂油气藏的油气分布、油气性质、运聚成藏配置条件和油气充注过程，认为研究区存在垂向充注、侧向运移主导型和垂向充注-侧向运移复合型3种充注模式(图12)。垂向充注

型最常见，一般出现在具有一定通源性、输导性和储集性的挤压段和拉分段，往往在平面上形成点状或斑状的油气分布(图12a)；侧向运移主导型主要出现在极弱通源但储集体侧向连通性较好的平移段，往往能够形成带状的连片油气藏(图12c)；垂向充注-侧向运移复合型出现在应力分段复杂的断裂带，在挤压段和拉分

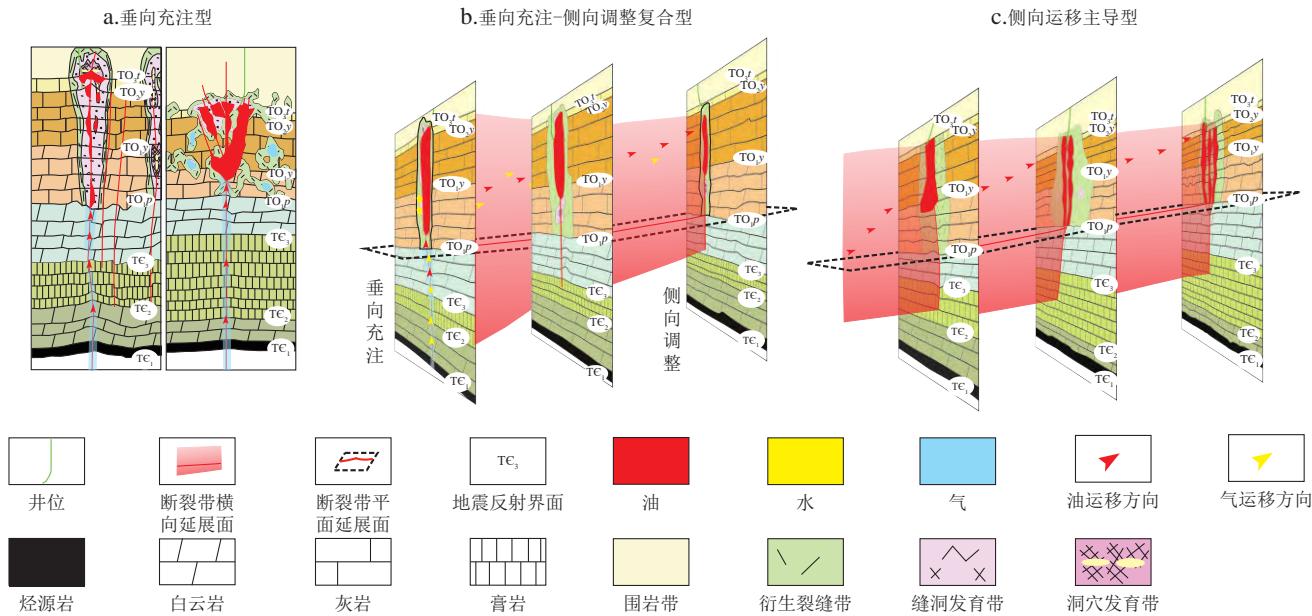


图12 富满地区典型走滑断裂带油气充注模式

Fig. 12 Hydrocarbon charging models in typical strike-slip fault zones in the Fuman area

段的强通源部位以垂向充注为主,在以平移段为主的弱通源部位,油气出现一定程度的侧向运移(图12b)。

4.4 油气性质与富集程度主控因素

烃源岩条件是富满地区油气成藏基础。前人通过将富满地区奥陶系原油与塔北隆起轮探1井玉尔吐斯组烃源岩三环萜烷和甾烷等生物标志化合物进行对比认为,富满地区的油气主要来自玉尔吐斯组,阿满过渡带位于烃源岩中心,烃源岩厚度整体在100~200 m,平均超过80 m;总有机碳含量(TOC)在7%~14%,平均12.1%;有机质热演化程度相对较高,等效镜质体反射率(R_o)介于1.5%~1.8%;有机质类型以I型和II₁型干酪根为主,整体达到了优质烃源岩的标准。与整个塔北隆起相比,研究区内烃源岩品质差异相对较小,烃源岩特征相对均一,受地温梯度的影响,区域内东部和西部、南部和北部的烃源岩热演化程度具有一定差异,对断裂带间的油气分布和富集具有一定程度影响。在研究区内,烃源岩品质整体较好,生烃能力均较强,特别在同一断裂带相邻部位,其烃源岩品质和特征基本一致,油气分布和富集程度受烃源岩的影响较小,而与油气的充注期次、运移及聚集条件密切相关。

在垂向充注型油气藏中,油气性质差异主要受烃源岩热演化过程及油气充注期次的控制,本质上是受走滑断裂带的活动期次和过程控制。油气富集程度本质上是通源性、储集性和输导性三者耦合的结果

(图13a—c)。通过利用加权法将三要素进行耦合,得到运聚成藏配置关系的综合定量判识指标——优势系数[公式(1)],该指标与油气产量呈较为明显的正相关关系(图13d)。

$$\Omega = Sr_s + Tr_T + Rr_R \quad (1)$$

式中: Ω 为优势系数,无量纲; S 为通源性强度,无量纲; T 为输导性强度,无量纲; R 为储集系数,无量纲; r_s, r_T, r_R 分别为通源性、输导性和储集性与油气产量相关性归一化后的权重系数,无量纲。

通过主因子分析方法分别提取与通源性、输导性和储集性相关的烃源岩地层变形强度、烃源岩层断距、膏岩层变形强度、膏岩层断距、膏岩层厚度和储集系数6个定量参数,分析它们与折日油气产量和累积油气产量的皮尔逊相关性(表3),得到6种主成分,所构建的前3种主成分即能反映油气富集程度主要变化[公式(2)—公式(4);表4],占比最高的主成分1主要与断裂通源性和输导性密切关联,次之的主成分2与储集性密切关联,主成分3则是由通源性、输导性和储集性三者共同控制,这说明油气在断裂带中的运移能力是研究区油气藏成藏和富集的最重要控制因素,其次为储集性。通过分析3种主成分与油气产量的相关性,得到断裂带油气富集控制因素的综合评分指标[公式(5)]。

在侧向运移型油气藏中,储集体的连通性控制了油气侧向运移方向和运移程度,影响了油气性质在断裂内的变化规律,而储集体的规模是富集程度的关键控制因素(图13e)。

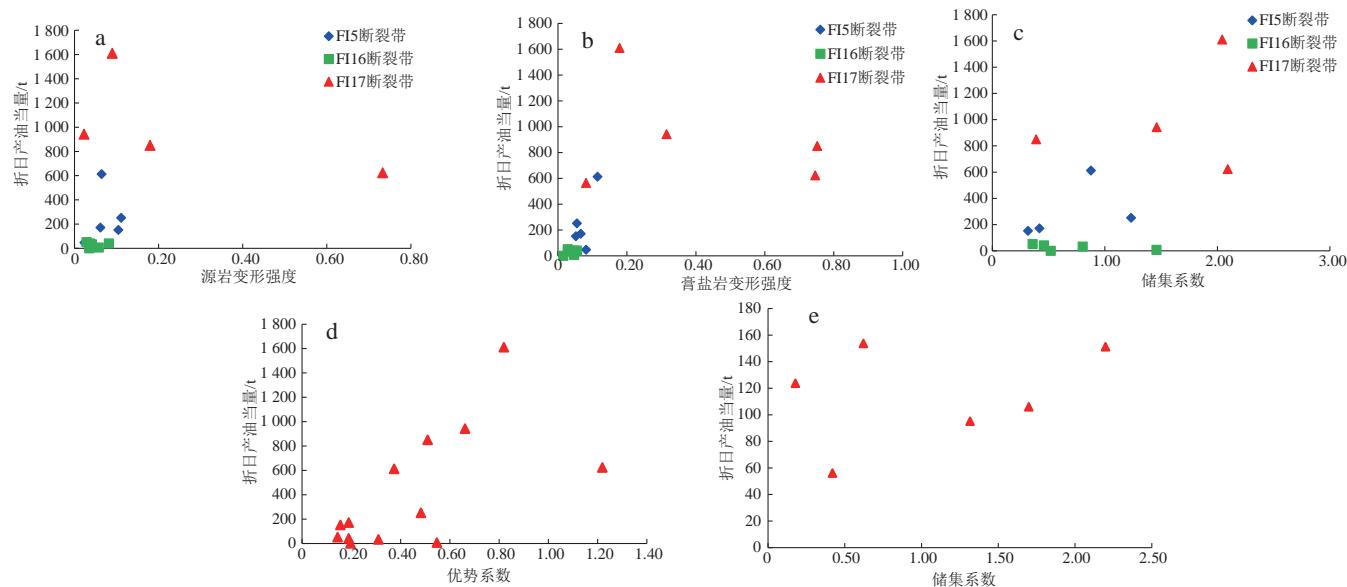


图13 富满地区走滑断裂带运聚成藏要素对油气富集程度的影响

Fig. 13 Influence of factors controlling hydrocarbon migration and accumulation on hydrocarbon enrichment in strike-slip fault zones in the Fuman area

a. 烃源岩层变形强度与折日产油气当量关系; b. 膏盐岩层变形强度与折日产油气当量关系; c. 储集系数与折日产油气当量关系; d. 垂向充注型油气藏优势系数与折日油气产量关系; e. 侧向运移调整主导型油气藏储集系数与折日产油当量关系

表3 富满地区断裂带油气成藏运聚条件参数与油气富集程度的皮尔逊相关性

Table 3 Pearson correlations between parameters for hydrocarbon migration and accumulation and the degree of hydrocarbon enrichment in strike-slip fault zones in the Fuman area

成藏运聚条件参数		折日产油气当量	累计产油	累计产气	累计产油气当量
源岩变形强度	皮尔逊相关系数	0.274	0.621**	0.732**	0.667**
	显著性水平(双尾)	0.304	0.008	0.001	0.003
源岩断距/m	皮尔逊相关系数	0.068	0.143	0.136	0.144
	显著性水平(双尾)	0.803	0.583	0.604	0.582
膏盐岩变形强度	皮尔逊相关系数	0.418*	0.183	0.354	0.231
	显著性水平(双尾)	0.042	0.380	0.082	0.266
膏盐岩断距/m	皮尔逊相关系数	0.507*	0.299	0.516**	0.361
	显著性水平(双尾)	0.012	0.147	0.008	0.076
膏盐岩厚度/m	皮尔逊相关系数	0.767**	0.044	0.219	0.091
	显著性水平(双尾)	0	0.834	0.292	0.666
储集系数	皮尔逊相关系数	0.355	0.262	0.300	0.277
	显著性水平(双尾)	0.125	0.251	0.187	0.224

注：“*”和“**”代表成藏运聚条件参数与油气富集程度的相关性大小，依次递增。

表4 富满地区断裂带油气成藏运聚条件参数6种主成分特征值及其方差百分比

Table 4 Characteristic values and variance percentages of six principal components of the hydrocarbon migration and accumulation parameters in strike-slip fault zones in the Fuman area

主成分编号	初始特征值	方差百分比/%	累积百分比/%
1	3.682	61.364	61.364
2	1.084	18.070	79.434
3	0.546	9.103	88.537
4	0.500	8.327	96.864
5	0.127	2.119	98.983
6	0.061	1.017	100.000

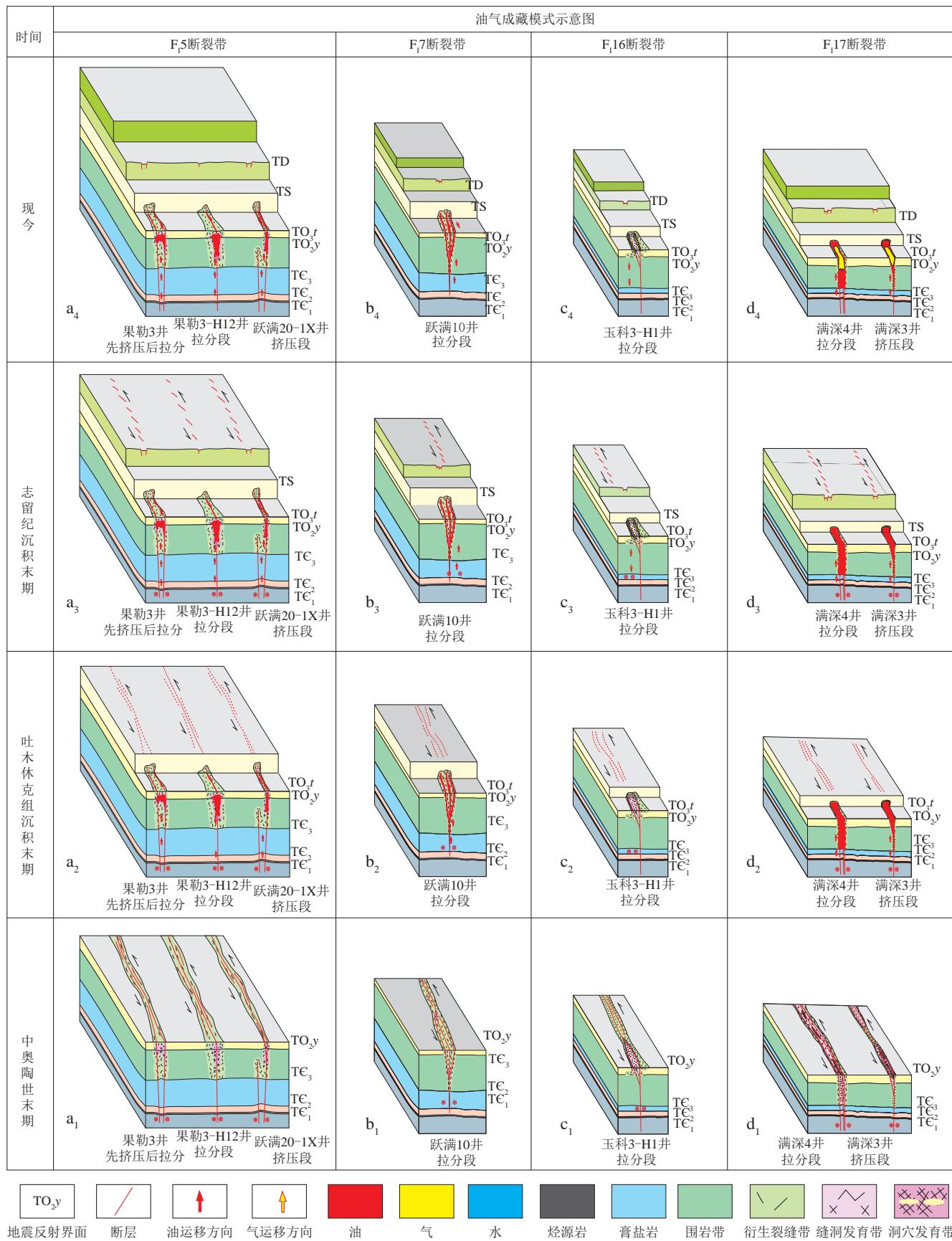


图14 富满地区走滑断裂带油气成藏模式

Fig. 14 Hydrocarbon accumulation patterns of strike-slip fault zones in the Fuman area

$$\begin{aligned} y_1 = & 0.467x_1 + 0.462x_2 + 0.452x_3 + 0.430x_4 + \\ & 0.362x_5 + 0.217x_6 \end{aligned} \quad (2)$$

$$\begin{aligned} y_2 = & -0.132x_1 + 0.127x_2 + 0.296x_3 - 0.363x_4 - \\ & 0.391x_5 + 0.771x_6 \end{aligned} \quad (3)$$

$$\begin{aligned} y_3 = & 0.329x_1 - 0.525x_2 - 0.447x_3 + 0.388x_4 + \\ & 0.037x_5 + 0.514x_6 \end{aligned} \quad (4)$$

$$y = 0.6136y_1 + 0.1807y_2 + 0.0910y_3 \quad (5)$$

式中: x_1 代表烃源岩层变形强度,无量纲; x_2 代表烃源岩层断距,m; x_3 代表膏盐岩变形强度,无量纲; x_4 代表膏盐岩断距,m; x_5 代表膏盐岩厚度,m; x_6 代表储集系数,无量纲; y 为主成分总得分值; y_1 为主成分1得分值; y_2 为主成分2得分值; y_3 为主成分3得分值。

垂向充注断裂带和垂向充注-侧向运移复合型断裂带的油气运聚条件综合得分与油气富集程度的相关性较好,皮尔逊相关系数基本都大于0.50,显著性水平大部分低于0.05。

4.5 油气差异运聚成藏模式探讨

走滑断裂是研究区油气成藏的基础,其演化过程决定了油气充注期次及其差异,演化强度与特征控制了通源性、输导性和储集性的耦合关系,影响了油气充注模式及富集程度。富满地区F₅断裂带为早-中期充注、通源性-输导性-储集性差异配置、点状分散聚集的成熟原油成藏模式(图14a),F₇断裂带为早-中期充注、油气侧向运移、条带状连片聚集的高成熟原油成藏模式(图14b),F₁₆断裂带为晚期充注主导、通源性-输导性差异配置、斑点状分散式聚集的高成熟凝析气成藏模式(图14c),F₁₇断裂带为晚期充注主导、通源性-储集性差异配置、带状-点状复杂聚集的高成熟凝析油气成藏模式(图14d)。

5 结论

1) 走滑断裂带特征及其演化过程是富满地区超深层碳酸盐岩油气藏油气成藏的关键,研究区形成了走滑断裂差异演化控制下的连锁式差异成藏模式。富满地区走滑断裂之间与内部演化过程差异明显,形成了早、中寒武世伸展或弱挤压,晚寒武世—中奥陶世末期压扭、增强伸展或平移走滑,晚奥陶世末—中泥盆世定型、继承性发育或张扭反转多种演化模式。

2) 差异演化导致了走滑断裂带的几何结构特征差别,控制了通源-输导-储集的运聚成藏条件配置关系,F₅断裂带受断裂强差异演化影响,存在强-中-中、弱-中-差、中-强-中、中-中-差等多种配置,油气运移

以垂向充注型为主;F₇断裂带活动性持续较强,形成强-强-优、强-强-中配置关系,油气运移以垂向充注-侧向调整复合型为主;F₇断裂带和F₁₆断裂带演化差异较小,运聚配置关系差异较小,F₇断裂带以中-强输导、中-差储集为主,油气以侧向运移主导型为主;F₁₆断裂带则以中通源、弱输导、中-差储集为主,油气垂向充注为主。

3) 走滑断裂演化过程差异与生排烃期次的耦合关系很大程度上影响了油气性质,晚期西部断裂带活动性整体比东部断裂带差,晚期高成熟天然气充注东部断裂带,形成高成熟度、低密度、气藏和凝析气藏。断裂带内不同部位演化过程的差异,导致断裂内油气性质变化规律复杂。

4) 在垂向充注型油气藏中通源性、输导性和储集性耦合控制了油气的富集程度,油气充注期次决定了油气物理化学性质,而侧向运移主导型油气藏中储集性规模及其侧向连通性分别控制了油气富集程度及油气性质变化。

参 考 文 献

- [1] EHRENBERG S N, NADEAU P H, STEEN Ø. Petroleum reservoir porosity versus depth: Influence of geological age [J]. AAPG Bulletin, 2009, 93(10): 1281–1296.
- [2] 贾承造, 张水昌. 中国海相超深层油气形成[J]. 地质学报, 2023, 97(9): 2775–2801.
JIA Chengzao, ZHANG Shuichang. The formation of marine ultra-deep petroleum in China [J]. Acta Geologica Sinica, 2023, 97(9): 2775–2801.
- [3] 赵喆. 近10年全球油气勘探特征分析及启示[J]. 石油科技论坛, 2019, 38(3): 58–64.
ZHAO Zhe. Analysis of global oil and gas exploration characteristics during the past decade [J]. Petroleum Science and Technology Forum, 2019, 38(3): 58–64.
- [4] 焦方正. 塔里木盆地顺托果勒地区北东向走滑断裂带的油气勘探意义[J]. 石油与天然气地质, 2017, 38(5): 831–839.
JIAO Fangzheng. Significance of oil and gas exploration in NE strike-slip fault belts in Shuntuogule area of Tarim Basin [J]. Oil & Gas Geology, 2017, 38(5): 831–839.
- [5] 罗晓容, 杨海军, 王震亮, 等. 深层—超深层碎屑岩储层非均质性特征与油气成藏模式[J]. 地质学报, 2023, 97(9): 2802–2819.
LUO Xiaorong, YANG Haijun, WANG Zhenliang, et al. Heterogeneity characteristics of clastic reservoirs and hydrocarbon accumulation mode in deep-ultradeep basins [J]. Acta Geologica Sinica, 2023, 97(9): 2802–2819.
- [6] 郑和荣, 胡宗全, 云露, 等. 中国海相克拉通盆地内部走滑断裂发育特征及控藏作用[J]. 地学前缘, 2022, 29(6):

- 224–238.
- ZHENG Herong, HU Zongquan, YUN Lu, et al. Strike-slip faults in marine cratonic basins in China: Development characteristics and controls on hydrocarbon accumulation [J]. *Earth Science Frontiers*, 2022, 29(6): 224–238.
- [7] 杨海军, 邓兴梁, 张银涛, 等. 塔里木盆地满深1井奥陶系超深断控碳酸盐岩油气藏勘探重大发现及意义[J]. 中国石油勘探, 2020, 25(3): 13–23.
- YANG Haijun, DENG Xingliang, ZHANG Yintao, et al. Great discovery and its significance of exploration for Ordovician ultra-deep fault-controlled carbonate reservoirs of Well Manshen 1 in Tarim Basin [J]. *China Petroleum Exploration*, 2020, 25(3): 13–23.
- [8] 张水昌, 苏劲, 张斌, 等. 塔里木盆地深层海相轻质油/凝析油的成因机制与控制因素[J]. 石油学报, 2021, 42(12): 1566–1580.
- ZHANG Shuichang, SU Jin, ZHANG Bin, et al. Genetic mechanism and controlling factors of deep marine light oil and condensate oil in Tarim Basin [J]. *Acta Petrolei Sinica*, 2021, 42(12): 1566–1580.
- [9] 田军, 杨海军, 朱永峰, 等. 塔里木盆地富满油田成藏地质条件及勘探开发关键技术[J]. 石油学报, 2021, 42(8): 971–985.
- TIAN Jun, YANG Haijun, ZHU Yongfeng, et al. Geological conditions for hydrocarbon accumulation and key technologies for exploration and development in Fuman Oilfield, Tarim Basin [J]. *Acta Petrolei Sinica*, 2021, 42(8): 971–985.
- [10] 邓尚, 李慧莉, 张仲培, 等. 塔里木盆地顺北及邻区主干走滑断裂带差异活动特征及其与油气富集的关系[J]. 石油与天然气地质, 2018, 39(5): 878–888.
- DENG Shang, LI Huili, ZHANG Zhongpei, et al. Characteristics of differential activities in major strike-slip fault zones and their control on hydrocarbon enrichment in Shunbei area and its surroundings, Tarim Basin [J]. *Oil & Gas Geology*, 2018, 39(5): 878–888.
- [11] 邓尚, 刘雨晴, 刘军, 等. 克拉通盆地内部走滑断裂发育、演化特征及其石油地质意义:以塔里木盆地顺北地区为例[J]. 大地构造与成矿学, 2021, 45(6): 1111–1126.
- DENG Shang, LIU Yuqing, LIU Jun, et al. Structural styles and evolution models of intracratonic strike-slip faults and the implications for reservoir exploration and appraisal: A case study of the Shunbei area, Tarim Basin [J]. *Geotectonica et Metallogenia*, 2021, 45(6): 1111–1126.
- [12] 韩剑发, 苏洲, 陈利新, 等. 塔里木盆地台盆区走滑断裂控储作用及勘探潜力[J]. 石油学报, 2019, 40(11): 1296–1310.
- HAN Jianfa, SU Zhou, CHEN Lixin, et al. Reservoir-controlling and accumulation-controlling of strike-slip faults and exploration potential in the platform of Tarim Basin [J]. *Acta Petrolei Sinica*, 2019, 40(11): 1296–1310.
- [13] 黄诚, 云露, 曹自成, 等. 塔里木盆地顺北地区中-下奥陶统“断控”缝洞系统划分与形成机制[J]. 石油与天然气地质, 2022, 43(1): 54–68.
- HUANG Cheng, YUN Lu, CAO Zicheng, et al. Division and formation mechanism of fault-controlled fracture-vug system of the Middle-to-Lower Ordovician, Shunbei area, Tarim Basin [J]. *Oil & Gas Geology*, 2022, 43(1): 54–68.
- [14] 林波, 张旭, 况安鹏, 等. 塔里木盆地走滑断裂构造变形特征及油气意义——以顺北地区1号和5号断裂为例[J]. 石油学报, 2021, 42(7): 906–923.
- LIN Bo, ZHANG Xu, KUANG Anpeng, et al. Structural deformation characteristics of strike-slip faults in Tarim Basin and their hydrocarbon significance: A case study of No. 1 fault and No. 5 fault in Shunbei area [J]. *Acta Petrolei Sinica*, 2021, 42(7): 906–923.
- [15] 云露, 邓尚. 塔里木盆地深层走滑断裂差异变形与控储控藏特征——以顺北油气田为例[J]. 石油学报, 2022, 43(6): 770–787.
- YUN Lu, DENG Shang. Structural styles of deep strike-slip faults in Tarim Basin and the characteristics of their control on reservoir formation and hydrocarbon accumulation: A case study of Shunbei oil and gas field [J]. *Acta Petrolei Sinica*, 2022, 43(6): 770–787.
- [16] 马永生, 蔡勋育, 李慧莉, 等. 深层-超深层碳酸盐岩储层发育机理新认识与特深层油气勘探方向[J]. 地学前缘, 2023, 30(6): 1–13.
- MA Yongsheng, CAI Xunyu, LI Huili, et al. New insights into the formation mechanism of deep-ultra-deep carbonate reservoirs and the direction of oil and gas exploration in extra-deep strata [J]. *Earth Science Frontiers*, 2023, 30(6): 1–13.
- [17] 宋兴国, 陈石, 杨明慧, 等. 塔里木盆地富满油田F₁₆断裂发育特征及其对油气分布的影响[J]. 岩性油气藏, 2023, 35(3): 99–109.
- SONG Xingguo, CHEN Shi, YANG Minghui, et al. Development characteristics of F₁₆ fault in Fuman Oilfield of Tarim Basin and its influence on oil and gas distribution [J]. *Lithologic Reservoirs*, 2023, 35(3): 99–109.
- [18] 王清华. 塔里木盆地17号走滑断裂带北段差异变形与演化特征[J]. 现代地质, 2023, 37(5): 1136–1145.
- WANG Qinghua. Differential deformation and evolution characteristics of the No. 17 strike-slip fault zone in the Tarim Basin [J]. *Geoscience*, 2023, 37(5): 1136–1145.
- [19] 杨德彬, 鲁新便, 高志前, 等. 塔北深层海相碳酸盐岩溶断体成藏认识及油藏特征[J]. 地学前缘, 2023, 30(4): 43–50.
- YANG Debin, LU Xinbian, GAO Zhiqian, et al. Hydrocarbon accumulation and reservoir characteristics of deep marine fault-karst reservoirs in northern Tarim Basin [J]. *Earth Science Frontiers*, 2023, 30(4): 43–50.
- [20] 王清华, 蔡振忠, 张银涛, 等. 塔里木盆地超深层走滑断裂油

- 气藏研究进展与趋势[J]. 新疆石油地质, 2024, 45(4): 379-386.
- WANG Qinghua, CAI Zhenzhong, ZHANG Yintao, et al. Research progress and trend of ultra-deep strike-slip fault-controlled hydrocarbon reservoirs in Tarim Basin [J]. Xinjiang Petroleum Geology, 2024, 45(4): 379-386.
- [21] 杨海军, 能源, 邵龙飞, 等. 塔里木盆地台盆区走滑断裂带多层叠加样式及石油地质意义[J]. 新疆石油地质, 2024, 45(4): 387-400.
- YANG Haijun, NENG Yuan, SHAO Longfei, et al. Multilayer superimposition patterns of strike-slip fault zones and their petroleum geological significance in platform area, Tarim Basin [J]. Xinjiang Petroleum Geology, 2024, 45(4): 387-400.
- [22] 韩强, 云露, 蒋华山, 等. 塔里木盆地顺北地区奥陶系油气充注过程分析[J]. 吉林大学学报(地球科学版), 2021, 51(3): 645-658.
- HAN Qiang, YUN Lu, JIANG Huashan, et al. Marine oil and gas filling and accumulation process in the north of Shuntuoguo area in northern Tarim Basin [J]. Journal of Jilin University (Earth Science Edition), 2021, 51(3): 645-658.
- [23] 史集建, 张璐, 林潼, 等. 塔里木盆地中下寒武统膏质白云岩盖层突破压力预测方法[J]. 大庆石油地质与开发, 2024, 43(5): 22-31.
- SHI Jijian, ZHANG Lu, LIN Tong, et al. Prediction method for breakthrough pressure capability of gypsum dolomite caprock of Middle and Lower Cambrian in Tarim Basin [J]. Petroleum Geology & Oilfield Development in Daqing, 2024, 43(5): 22-31.
- [24] 陈烈, 邵皓枫, 尹贝, 等. 顺北油气田超深井目的层测井施工技术探讨[J]. 石油地质与工程, 2024, 38(3): 117-121.
- CHEN Lie, SHAO Haofeng, YIN Bei, et al. Exploration of logging construction technology for target layers in ultra deep wells in Shunbei oil and gas field [J]. Petroleum Geology and Engineering, 2024, 38(3): 117-121.
- [25] 张银涛, 陈石, 刘强, 等. 塔里木盆地富满油田F₁₉断裂发育特征及演化模式[J]. 现代地质, 2023, 37(2): 283-295.
- ZHANG Yintao, CHEN Shi, LIU Qiang, et al. Development characteristics and evolution model of F₁₉ fault in Fuman Oilfield, Tarim Basin [J]. Geoscience, 2023, 37(2): 283-295.
- [26] 朱秀香, 曹自成, 隆辉, 等. 塔里木盆地顺北地区走滑断裂带压扭段和张扭段油气成藏实验模拟及成藏特征研究[J]. 地学前缘, 2023, 30(6): 289-304.
- ZHU Xiuxiang, CAO Zicheng, LONG Hui, et al. Experimental simulation and characteristics of hydrocarbon accumulation in strike-slip fault zone in Shunbei area, Tarim Basin [J]. Earth Science Frontiers, 2023, 30(6): 289-304.
- [27] 李斌, 姜潇俊, 赵星星, 等. 塔里木盆地台盆过渡带多相态油气藏成因及差异富集模式——以玉科地区奥陶系为例[J]. 石油学报, 2023, 44(5): 794-808.
- LI Bin, JIANG Xiaojun, ZHAO Xingxing, et al. Genesis and differential enrichment model of multiphase reservoirs in platform-basin transitional zone of Tarim Basin: A case study of the Ordovician in Yuke area [J]. Acta Petrolei Sinica, 2023, 44(5): 794-808.
- [28] 马庆佑, 曹自成, 蒋华山, 等. 塔河—顺北地区走滑断裂带的通源性及其与油气富集的关系[J]. 海相油气地质, 2020, 25(4): 327-334.
- MA Qingyou, CAO Zicheng, JIANG Huashan, et al. Source-connectivity of strike slip fault zone and its relationship with oil and gas accumulation in Tahe-Shunbei area, Tarim Basin [J]. Marine Origin Petroleum Geology, 2020, 25(4): 327-334.
- [29] 马永生, 蔡勋育, 云露, 等. 塔里木盆地顺北超深层碳酸盐岩油气田勘探开发实践与理论技术进展[J]. 石油勘探与开发, 2022, 49(1): 1-17.
- MA Yongsheng, CAI Xunyu, YUN Lu, et al. Practice and theoretical and technical progress in exploration and development of Shunbei ultra-deep carbonate oil and gas field, Tarim Basin, NW China [J]. Petroleum Exploration and Development, 2022, 49(1): 1-17.
- [30] 田鹏, 马庆佑, 吕海涛. 塔里木盆地北部跃参区块走滑断裂对油气成藏的控制[J]. 石油实验地质, 2016, 38(2): 156-161.
- TIAN Peng, MA Qingyou, LYU Haitao. Strike-slip faults and their controls on hydrocarbon reservoirs in the Yuecan block of the northern Tarim Uplift, Tarim Basin [J]. Petroleum Geology and Experiment, 2016, 38(2): 156-161.
- [31] 王清华, 杨海军, 李勇, 等. 塔里木盆地富满大型碳酸盐岩油气聚集区走滑断裂控储模式[J]. 地学前缘, 2022, 29(6): 239-251.
- WANG Qinghua, YANG Haijun, LI Yong, et al. Control of strike-slip fault on the large carbonate reservoir in Fuman, Tarim Basin—A reservoir model [J]. Earth Science Frontiers, 2022, 29(6): 239-251.
- [32] 邓铭哲, 蔡苑睿, 陆建林, 等. 走滑断裂演化程度的表征参数研究[J]. 石油实验地质, 2023, 45(5): 1007-1015.
- DENG Mingzhe, CAI Pengrui, LU Jianlin, et al. Characterization parameters of the evolution degree of strike-slip faults [J]. Petroleum Geology and Experiment, 2023, 45(5): 1007-1015.
- [33] 冯建伟, 郭宏辉, 汪如军, 等. 塔里木盆地塔北地区深层走滑断裂分段性成因机制[J]. 地球科学, 2023, 48(7): 2506-2519.
- FENG Jianwei, GUO Honghui, WANG Ruijun, et al. Segmentation genesis mechanism of strike-slip fracture of deep carbonate rocks in Tabei area, Tarim Basin [J]. Earth Science, 2023, 48(7): 2506-2519.
- [34] 李凤磊, 林承焰, 张国印, 等. 塔北地区多期走滑断裂地球物理响应特征及精细识别[J]. 中国石油大学学报(自然科学版), 2024, 48(3): 1-14.
- LI Fenglei, LIN Chengyan, ZHANG Guoyin, et al.

- Characteristics of geophysical response and fine identification of multi-stage strike-slip fault in Tabei area [J]. Journal of China University of Petroleum (Edition of Natural Science), 2024, 48 (3): 1–14.
- [35] 何治亮, 赵向原, 张文彪, 等. 深层-超深层碳酸盐岩储层精细地质建模技术进展与攻关方向[J]. 石油与天然气地质, 2023, 44(1): 16–33.
HE Zhiliang, ZHAO Xiangyuan, ZHANG Wenbiao, et al. Progress and direction of geological modeling for deep and ultra-deep carbonate reservoirs [J]. Oil & Gas Geology, 2023, 44(1): 16–33.
- [36] 宋兴国, 陈石, 谢舟, 等. 塔里木盆地富满油田东部走滑断裂发育特征与油气成藏[J]. 石油与天然气地质, 2023, 44(2): 335–349.
SONG Xingguo, CHEN Shi, XIE Zhou, et al. Strike-slip faults and hydrocarbon accumulation in the eastern part of Fuman Oilfield, Tarim Basin [J]. Oil & Gas Geology, 2023, 44(2): 335–349.
- [37] 云露, 朱秀香. 一种新型圈闭: 断控缝洞型圈闭[J]. 石油与天然气地质, 2022, 43(1): 34–42.
YUN Lu, ZHU Xiuxiang. A new trap type: Fault-controlled fracture-vuggy trap [J]. Oil & Gas Geology, 2022, 43(1): 34–42.
- [38] 付晓飞, 冯军, 王海学, 等. 走滑断裂“分期-异向”变形过程砂箱物理模拟: 以塔里木盆地顺北5号断层北段为例[J]. 地球科学, 2023, 48(6): 2104–2116.
FU Xiaofei, FENG Jun, WANG Haixue, et al. Sandbox physical simulation on “different period-different direction” deformation process of strike-slip faults: A case study of northern segment of Shunbei No. 5 fault in Tarim Basin [J]. Earth Science, 2023, 48(6): 2104–2116.
- [39] 吴鲜, 李丹, 朱秀香, 等. 塔里木盆地顺北油气田地温场对奥陶系超深层油气的影响——以顺北5号走滑断裂带为例[J]. 石油实验地质, 2022, 44(3): 402–412.
WU Xian, LI Dan, ZHU Xiuxiang, et al. Influence of geothermal field on ultra-deep Ordovician oil and gas in Shunbei field, Tarim Basin: A case study of Shunbei No. 5 strike-slip fault [J]. Petroleum Geology and Experiment, 2022, 44(3): 402–412.
- [40] 赵永强, 云露, 王斌, 等. 塔里木盆地塔河油田中西部奥陶系油气成藏主控因素与动态成藏过程[J]. 石油实验地质, 2021, 43(5): 758–766.
ZHAO Yongqiang, YUN Lu, WANG Bin, et al. Main constrains and dynamic process of Ordovician hydrocarbon accumulation, central and western Tahe Oil Field, Tarim Basin [J]. Petroleum Geology and Experiment, 2021, 43(5): 758–766.
- [41] 汪如军, 王轩, 邓兴梁, 等. 走滑断裂对碳酸盐岩储层和油气藏的控制作用——以塔里木盆地北部坳陷为例[J]. 天然气工业, 2021, 41(3): 10–20.
WANG Rujun, WANG Xuan, DENG Xingliang, et al. Control effect of strike-slip faults on carbonate reservoirs and hydrocarbon accumulation: A case study of the northern depression in the Tarim Basin [J]. Natural Gas Industry, 2021, 41(3): 10–20.
- [42] 李兵, 罗枭, 王轩, 等. 塔里木盆地富满油田深区块南北向走滑断裂形成机制[J/OL]. 大庆石油地质与开发: 1–11[2024–06–25]. <https://doi.org/10.19597/J.ISSN.1000-3754.202309027>.
LI Bing, LUO Xiao, WANG Xuan, et al. Formation mechanism of north-south strike slip fault in Manshen block of Fuman Oilfield, Tarim Basin [J/OL]. Petroleum Geology & Oilfield Development in Daqing: 1–11[2024–06–25]. <https://doi.org/10.19597/J.ISSN.1000-3754.202309027>.
- [43] 田军, 王清华, 杨海军, 等. 塔里木盆地油气勘探历程与启示[J]. 新疆石油地质, 2021, 42(3): 272–282.
TIAN Jun, WANG Qinghua, YANG Haijun, et al. Petroleum exploration history and enlightenment in Tarim Basin [J]. Xinjiang Petroleum Geology, 2021, 42(3): 272–282.
- [44] 贾承造, 马德波, 袁敬一, 等. 塔里木盆地走滑断裂构造特征、形成演化与成因机制[J]. 天然气工业, 2021, 41(8): 81–91.
JIA Chengzao, MA Debo, YUAN Jingyi, et al. Structural characteristics, formation & evolution and genetic mechanisms of strike-slip faults in the Tarim Basin [J]. Natural Gas Industry, 2021, 41(8): 81–91.
- [45] 田方磊, 何登发, 陈槚俊, 等. 塔里木盆地顺北5号走滑断裂带北-中段构造特征与多期构造叠加演化时-空序列[J]. 地球科学, 2023, 48(6): 2117–2135.
TIAN Fanglei, HE Dengfa, CHEN Jiajun, et al. Northern and central segments of Shunbei No. 5 strike-slip fault zone in Tarim Basin: Structural characteristics and spatio-temporal evolution process [J]. Earth Science, 2023, 48(6): 2117–2135.
- [46] 张红波, 周雨双, 沙旭光, 等. 塔里木盆地顺北5号走滑断裂隆起段发育特征与演化机制[J]. 石油与天然气地质, 2023, 44(2): 321–334.
ZHANG Hongbo, ZHOU Yushuang, SHA Xuguang, et al. Development characteristics and evolution mechanism of the uplifted segment of the No. 5 strike-slip fault zone in Shunbei area, Tarim Basin [J]. Oil & Gas Geology, 2023, 44(2): 321–334.
- [47] 刘雨晴, 邓尚, 张继标, 等. 塔里木盆地顺北及邻区走滑断裂体系差异发育特征及成因机制探讨[J]. 地学前缘, 2023, 30(6): 95–109.
LIU Yuqing, DENG Shang, ZHANG Jibiao, et al. Characteristics and formation mechanism of the strike-slip fault networks in the Shunbei area and the surroundings, Tarim Basin [J]. Earth Science Frontiers, 2023, 30(6): 95–109.
- [48] 吴昌达, 赵学钦, 邬光辉, 等. 塔北跃满区块一间房组碳酸盐岩断控型储层特征及其分布规律[J]. 中国地质, 2024, 51(3): 762–779.
WU Changda, ZHAO Xueqin, WU Guanghui, et al. Characteristics and distribution of fault-controlled carbonate

- reservoirs in Yijianfang Formation of Yueman area, northern Tarim Basin[J]. Geology in China, 2024, 51(3): 762–779.
- [49] 罗彩明, 梁鑫鑫, 黄少英, 等. 塔里木盆地塔中隆起走滑断裂的三层结构模型及其形成机制[J]. 石油与天然气地质, 2022, 43(1): 118–131, 148.
LUO Caiming, LIANG Xinxin, HUANG Shaoying, et al. Three-layer structure model of strike-slip faults in the Tazhong Uplift and its formation mechanism[J]. Oil & Gas Geology, 2022, 43(1): 118–131, 148.
- [50] 李传新, 贾承造, 李本亮, 等. 塔里木盆地塔中低凸起北斜坡古生代断裂展布与构造演化[J]. 地质学报, 2009, 83(8): 1065–1073.
LI Chuanxin, JIA Chengzao, LI Benliang, et al. Distribution and tectonic evolution of the Paleozoic fault system, the north slope of Tazhong uplift, Tarim Basin[J]. Acta Geologica Sinica, 2009, 83(8): 1065–1073.
- [51] 李萌, 汤良杰, 漆立新, 等. 塔北隆起南坡差异构造演化及其对油气成藏的控制[J]. 天然气地球科学, 2015, 26(2): 218–228.
LI Meng, TANG Liangjie, QI Lixin, et al. Differential tectonic evolution and its controlling on hydrocarbon accumulation in the south slope of Tabei uplift[J]. Natural Gas Geoscience, 2015, 26(2): 218–228.
- [52] 汤良杰, 黄太柱, 邱海峻, 等. 塔里木盆地塔河地区海西晚期火山岩构造特征与油气成藏[J]. 地质学报, 2012, 86(8): 1188–1197.
TANG Liangjie, HUANG Taizhu, QIU Haijun, et al. The tectonic characteristics and hydrocarbon accumulation of Late Hercynian volcanic rocks in the Tahe area, Tarim Basin[J]. Acta Geologica Sinica, 2012, 86(8): 1188–1197.
- [53] 况安鹏, 余一欣, 朱秀香, 等. 塔里木盆地顺北地区11号走滑断裂带变形及其活动特征[J]. 现代地质, 2021, 35(6): 1809–1817.
KUANG Anpeng, YU Yixin, ZHU Xiuxiang, et al. Deformation and activity characteristics of the No. 11 strike-slip fault zone in the Shunbei area, Tarim Basin[J]. Geoscience, 2021, 35(6): 1809–1817.
- [54] 李映涛, 邓尚, 张继标, 等. 深层致密碳酸盐岩走滑断裂带核带结构与断控储集体簇状发育模式: 以塔里木盆地顺北4号断裂带为例[J]. 地学前缘, 2023, 30(6): 80–94.
LI Yingtao, DENG Shang, ZHANG Jibiao, et al. Fault zone architecture of strike-slip faults in deep, tight carbonates and development of reservoir clusters under fault control: A case study in Shunbei, Tarim Basin[J]. Earth Science Frontiers, 2023, 30(6): 80–94.
- [55] 李映涛, 漆立新, 张哨楠, 等. 塔里木盆地顺北地区中——下奥陶统断溶体储层特征及发育模式[J]. 石油学报, 2019, 40(12): 1470–1484.
LI Yingtao, QI Lixin, ZHANG Shaonan, et al. Characteristics and development mode of the Middle and Lower Ordovician fault-karst reservoir in Shunbei area, Tarim Basin[J]. Acta Petrolei Sinica, 2019, 40(12): 1470–1484.
- [56] 丛富云. 塔里木盆地塔北隆起中西部下古生界深层油气成藏过程[D]. 武汉: 中国地质大学, 2021.
CONG Fuyun. Hydrocarbon accumulation processes of the Lower Paleozoic deep reservoirs in the Central and Western part of Tabei uplift, Tarim Basin[D]. Wuhan: China University of Geosciences, 2021.
- [57] 李丹, 常健, 邱楠生, 等. 塔里木盆地顺北地区热演化及与超深层油气成藏的关系[C]//中国地球物理学会, 中国地震学会, 全国岩石学与地球动力学研讨会组委会, 等. 2020年中国地球科学联合学术年会论文集(十一), 重庆, 2020. 北京: 北京伯通电子出版社, 2020: 32.
LI Dan, CHANG Jian, QIU Nansheng, et al. Thermal evolution in Shunbei area of Tarim Basin and its relationship with ultra deep oil and gas accumulation [C]//Chinese Geophysical Society, Seismological Society of China, Organizing Committee of the National Symposium on Petrography and Geodynamics, et al. Proceedings of the 2020 China Earth Science Joint Academic Annual Conference (11), Chongqing, 2020. Beijing: Beijing Botong Digital Publishing House, 2020: 32.

(编辑 张玉银)